A formulation of membrane finite elements with true drilling rotation

The compatible triangular element

Djamel Boutagouga
Department of Civil Engineering, Laboratoire des Mines, University of Tebessa, Tebessa, Algeria

Received 14 December 2018
Revised 16 April 2019
17 June 2019
Accepted 17 June 2019

Abstract

Purpose – This paper aims to describe the formulation of a displacement-based triangular membrane finite element with true drilling rotational degree of freedom (DOF).

Design/methodology/approach – The presented formulation incorporates the true drilling rotation provided by continuum mechanics into the displacement field by way of using the polynomial interpolation. Unlike the linked interpolation, that uses a geometric transformation between displacement and vertex rotations, in this work, the interpolation of the displacement field in terms of nodal drilling rotations is obtained following an unusual approach that does not imply any presumed geometric transformation.

Findings – New relationship linking the mid-side normal displacement to corner node drilling rotations is derived. The resulting new element with true drilling rotation is compatible and does not include any problem-dependent parameter that may influence the results. The spurious zero-energy mode is stabilized in a careful way that preserves the true drilling rotational degrees of freedom (DOFs).

Originality/value – Several works dealing with membrane elements with vertex rotational DOFs have been published with improved convergence rate, however, owing to the need for incorporating rotations in the finite element meshes involving solids, shells and beam elements, having finite elements with true drilling rotational DOFs is more appreciated.

Keywords Drilling rotation, True drilling rotation, Drilling rotational DOF, Compatible triangular element, Membrane element, Shell element, Finite element

Paper type Research paper

1. Introduction

Flat shell finite elements are widely used in structural analysis of spatial shells and folded plates because of the formulation simplicity and numerical efficiency. However, this formulation that lies on the combination of membrane and plate bending elements lead to ill-conditioned or even singular stiffness matrices, whenever elements are coplanar or nearly so. That deficiency arises from the fact that conventional membrane elements make use of only the nodal translational degrees of freedom (DOFs).

In many practical engineering problems, the shell formulation must provide a complete description of the nodal translation and rotation fields, which requires the definition of six DOFs for each node including the rotation θ_z around the shell mid-surface normal. This in-plane rotational DOF, so-called "drilling rotation", has been introduced in shell elements formulation with various meanings to: evade stiffness matrix singularity, to improve convergence and to connect with other kinds of elements with rotational DOFs such as beam and plate elements.

To evade stiffness matrix singularity, Zienkiewicz *et al.* (1965), Zienkiewicz (1977), and Bathe and Ho (1981) proposed to use a fictitious rotational stiffness in the direction of this

Engineering Computations
Vol. 37 No. 1, 2020
pp. 203-236

0264-4401
DOI 10.1108/EC-12-2018-0572

DOF. The fictitious rotation must be defined in the way that it does not perturb the local equilibrium of the finite element. In addition, the sum of all additional terms must be null so, rigid rotations condition is always guaranteed. While this method satisfactorily overcomes the stiffness matrix singularity problem, unfortunately, the additional fictitious rotational stiffness has no physical interpretation.

Numerous efforts have been made to determine a rotational stiffness with physical interpretation by linking the in-plane rotational DOF to the displacement field of membrane elements. These elements are known as "membrane elements with drilling rotation". This feature has also been recognized as an attractive approach to achieve intermediate accuracy between linear and higher order elements with translational DOFs only while comprising a computational effort greatly less than higher order elements.

The idea of including in-plane normal-rotation DOF at corner nodes in membrane elements formulation is an old one. However, the first successful work was made by Allman (1984) and Carpenter *et al.* (1985) independently by introducing the concept of the vertex rotation into the "constant strain triangle". In these works, the coupling between the in-plane rotational DOF and the displacements is taken into account. However, the considered rotational DOF does not represent the true drilling rotation provided by continuum mechanics. The stiffness matrix was evaluated using a reduced integration scheme. The reduced integrated elements gave better results compared to the fully integrated elements, but they resulted in spurious zero energy modes. Bergan and Felippa (1985) have also introduced the in-plane rotational DOF using the free formulation (Bergan and Nygård, 1984). Incorporating the in-plane rotation as an additional DOF has also extended to quadrilateral membrane elements (Cook, 1986; Allman, 1988). Subsequently, many similar methods have been proposed for triangular and quadrilateral elements (Cook, 1987; MacNeal and Harder, 1988; Jaamei *et al.*, 1989; MacNeal, 1989; Cook, 1990; Cook, 1991; Allman, 1993; Cook, 1993; Cook, 1994). However, these elements all suffered from the serious drawback that they do not use the true drilling rotational DOF. They all incorporate the vertex rotational DOF instead. The main objective behind these elements was to avoid singularity problem and to improve convergence rate.

To address this deficiency, Ibrahimbegovic and co-authors (Ibrahimbegovic *et al.*, 1990; Ibrahimbegovic and Wilson, 1991) used a simplified variational formulation by Hughes and Brezzi (1989) to make the vertex rotation approaching the drilling rotation. In this formulation, the kinematic variables of displacement and rotation are separated by introducing both symmetric field for displacement and skew-symmetric field for drilling rotation. Several modified variational formulations have also been proposed and used (Simo *et al.*, 1992; Iura and Atluri,1992; Ibrahimbegovic and Frey, 1992; Ibrahimbegovic, 1993; Cazzani and Atluri, 1993).

Mixed and hybrid membrane elements using the Allman-type shape functions have been presented with varying degrees of success (Sze *et al.*, 1992; To and Liu, 1994; Piltner and Taylor, 1995; Piltner and Taylor, 2000; Geyer and Groenwold, 2002; Felippa, 2003; Pimpinelli, 2004; Choi *et al.*, 2006; Wisniewski and Turska, 2006; Wisniewski and Turska, 2008; Wisniewski and Turska, 2009; Kugler *et al.*, 2010).

Sabir (1985) derived rectangular and triangular non-conforming elements incorporating the in-plane rotation calculated through continuum mechanics by using a strain-based approach. Belarbi and Bourezane (2005), Rebiai and Belounar (2013); and Rebiai and Belounar (2014) used the same method in their works. However, numerical resets show that only rectangular elements provide good results. Moreover, these elements lack a consistent theoretical basis to ensure convergence.

Owing to the absence of an explicit methodology of incorporating the true drilling rotation into the in-plane displacement field, the linked interpolation concept proposed by Allman (1984) and Carpenter *et al.* (1985) even today represents the theoretical support for the development of several triangular and quadrangular membrane and shell elements (for instance, Cen *et al.*, 2011; Madeo *et al.*, 2012; Rezaiee-Pajand and Karkon, 2013; Madeo *et al.*, 2014; Xing and Zhou, 2016; Zouari *et al.*, 2016; Boutagouga and Djeghaba, 2016; Boutagouga, 2017; Rezaiee-Pajand and Yaghoobi, 2017; and Shang and Ouyang, 2018). The aim of these works was to improve the convergence rate of low order membrane elements. For the same purpose, Allman's interpolation has also been used in formulating tetrahedrons and hexahedron solid elements with rotational DOF (Yunus *et al.*, 1991; Pawlak *et al.*, 1991; Sze *et al.*, 1996; Sze and Pan, 2000: Nodargi *et al.*, 2016). These solid elements are demonstrated to be significantly better than the usual solid elements with translational DOFs only.

However, to form shell elements with compatible rotational DOFs of the other type of structural elements, the most important purpose is the formulation of membrane elements with true drilling rotational quantity. Having the true drilling rotation as nodal DOF will allow a shell finite element to compatibly connect with other kinds of elements with rotational DOFs such as beam and plate elements. In these cases, obtaining the true drilling rotation in the numerical analysis is most appreciated as the convergence rate.

Regarding the abundant literature dealing with membrane elements with vertex rotational DOFs in which the main goal was to improve the element's convergence rate, the elaboration of membrane elements with true drilling rotational DOFs becomes a more exhorting necessity. Hence, the main goal of this investigation is the derivation of a compatible triangular membrane element with true drilling rotational DOF, which equals the skew-symmetric part of the displacement gradient. Note that it is not the aim of the present work to enhance the convergence rate of the presented finite element.

2. A closer look at membrane elements with vertex rotation

The linked interpolation that found the support of membrane elements with rotational DOF consists of a geometric transformation relating the mid-side normal displacements in terms of corner displacements and rotations. The vertex rotation is geometrically interpolated in relation to the in-plane normal displacement at a mid-side node (k) between two nodes (i) and (j) (Figure 1) as:

$$P_k = \frac{l_{ij}}{8}(\omega_j - \omega_i) \tag{1}$$

where P_k is a vector quantity that stands for the mid-side node normal displacement due to the in-plane corner node vertex rotations. For simplicity, we will drop the vector notation in the sequel.

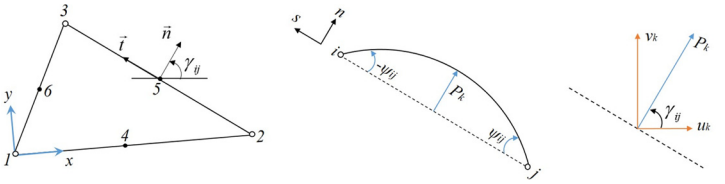

Figure 1. Transformation of the mid-side normal displacements in terms of the corner rotations

In Cartesian coordinates, the expressions for displacements u_k and v_k at mid-side nodes are obtained through the mid-side node normal displacement P_k and a coordinate transformation of directions between the systems $(x - y)$ and $(n - t)$. A schematic of the required coordinate transformation is shown in Figure 1, with $\psi_{ij} = 1/2(\omega_j - \omega_i)$. The transformation expression is:

$$\begin{Bmatrix} u_k \\ v_k \end{Bmatrix} = P_k \cdot \begin{Bmatrix} C_{ij} \\ S_{ij} \end{Bmatrix} \tag{2}$$

With this coordinate transformation, we can now write the quadratic displacement interpolation fields $u(\xi, \eta)$ and $v(\xi, \eta)$ inside the element in terms of nodal and mid-side displacement DOFs. For a triangular element, this interpolation yields:

$$\begin{Bmatrix} u \\ v \end{Bmatrix} = \sum_{i=1}^{3} N_i^e(\xi, \eta) \begin{Bmatrix} u_i \\ v_i \end{Bmatrix} + \sum_{k=4}^{6} NL_k^e(\xi, \eta) \cdot P_k \cdot \begin{Bmatrix} C_{ij} \\ S_{ij} \end{Bmatrix} \tag{3}$$

where $\{U_i\} = \begin{Bmatrix} u_i \\ v_i \end{Bmatrix}$ represents the nodal displacements vector. l_{ij}, C_{ij} and S_{ij} respectively represent the length and outward normal components of the edge located between nodes (i) and (j).

N_i^e is the shape functions of the "constant strain triangle", and NL_k^e is the quadratic shape functions of the "linear strain triangle".

However, in this formulation, the picked nodal rotational *DOF* represents the vertex rotation ω, which cannot represent the true drilling rotational DOF φ. In fact, Allman's linked interpolation considers the element as beams assembly hinged at corner nodes. If we consider a beam element with a quadratic interpolation through two corner nodes (i) and (j), and a mid-side node (k), the mid-side node normal displacement P_k can be expressed in terms of the displacement derivatives at corner nodes "ω_i and ω_j" by using equation (1). In Allman's interpolation, each mid-side displacement is related to the considered side rotation ψ_{ij}. This fact makes the three edges of the triangular element behave as a hinged beams assembly.

However, we are dealing with a planar *2D* element filled with a constitutive material between the edges, which dictates to the edges displacements to be inter-related to each other. In Allman's triangle, on the first hand, it is assumed that $P_k = \frac{l_{ij}}{8}(\omega_j - \omega_i)$. On the other hand, we can write:

$$(\omega_j - \omega_i) = \frac{8}{l_{ij}} P_k \tag{4}$$

By considering the three edges of the triangular element, we can write:

$$(\omega_2 - \omega_1) + (\omega_3 - \omega_2) + (\omega_1 - \omega_3) = 0 \tag{5}$$

By substituting equation (4) into equation (5) we get:

$$\frac{P_4}{l_{12}} + \frac{P_5}{l_{23}} + \frac{P_6}{l_{31}} = 0 \tag{6}$$

It is important here to make it clear that this relation between mid-side normal displacements is because of the adopted parabolic compatible interpolation of the edge normal displacement. As shown in Figure 2, the mid-side normal displacement of one edge (ij) have to satisfy some equilibrium condition together with the mid-side normal displacements of the two other edges (jl) and (li) in such a way that: $\psi_{ij} = \psi_{jl} + \psi_{li}$.

Then, in case when we are dealing with true drilling nodal rotations, how can we express these inter mid-side normal displacements relations, and how can we evaluate the mid-side normal displacements in terms of true drilling rotational *DOFs*? This fact, as we will see, constitutes the aim issue that faces the formulation of a plane element with true drilling rotation.

3. Formulation of the triangular element with true drilling rotation

The objective of this investigation is the formulation of a three-node triangular membrane element with true in-plane drilling rotation. The element's formulation deals with three DOFs per node (two nodal translation quantities, u_i and v_i, and one drilling rotation quantity φ_i) in a total of nine DOFs. This sought-after element needs to satisfy the following critical requirements:

- true drilling rotational DOF;
- conformity and reliability of interpolation; and
- no adjustable parameters.

The present element is formulated within the framework of the displacement approach. We have chosen to use the polynomial interpolation because it offers the possibility of a straightforward description of a higher-order displacement via the use of polynomial functions with priory unknown parameters. These parameters will subsequently be expressed in terms of nodal quantities. Hence, we aim here to avoid the use of any uncertain geometric transformations between mid-side displacements and corner rotations. As we will see, this choice allows the possibility of incorporating the true in-plan rotational *DOF* in the element's formulation by way of the definition provided by continuum mechanics as follows:

$$\varphi = \frac{1}{2}\left(\frac{\partial v}{\partial x} - \frac{\partial u}{\partial y}\right) \tag{7}$$

3.1 Basic assumptions

As a starting point, we have adopted the complete parabolic polynomial interpolation of the linear strain triangle (LST) element to be the basic frame of this investigation. The complete quadratic displacement can be expressed as:

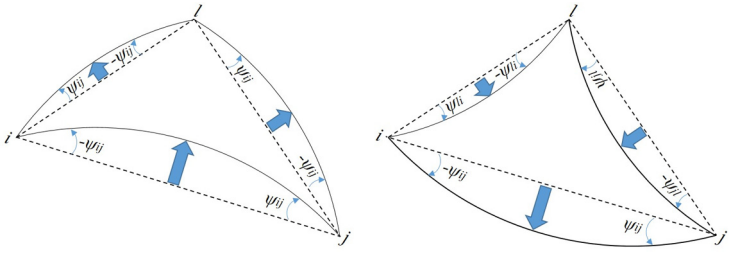

Figure 2.
Possible kinematics of an element with nodal rotations

$$\begin{cases} u = \lambda_1 + \lambda_2 x + \lambda_3 y + \lambda_4 x^2 + \lambda_5 xy + \lambda_6 y^2 \\ v = \lambda_7 + \lambda_8 x + \lambda_9 y + \lambda_{10} x^2 + \lambda_{11} xy + \lambda_{12} y^2 \end{cases} \tag{8}$$

However, this polynomial interpolation deals with 12 unknown constants (λ_i; for $i = 1 \ldots 12$) to be determined while we only have nine equations upraised from the nine nodal displacements (u_i, v_i and φ_i; for $i = 1 \ldots 3$). Thus, if we chose to work on a triangular element with the nine DOFs of the displacement formulation, the number of unknown parameters has to be reduced to nine.

To achieve this aim, we need to impose a kinematic restriction to equation (8), by assuming the normal displacement along the edge of the element to be a quadratic function, while the tangential component remains linear. This manipulation allows us to link the higher order displacement fields u and v to reduce the number of unknown constants λ_i in the interpolation of equation (8). Nevertheless, we will not assume any transformation that relates the mid-side normal displacements in terms of the corner displacements and rotations as usually done for membrane elements with vertex rotation. We are simply assuming that nodal rotations of nodes (i) and (j) provide only normal displacement along an edge (ij). The provided normal displacement at a mid-side node is noted P_k and it is given in equation (2).

3.2 Formulation of the displacement field

The displacement field in equation (8) can be split into linear and parabolic parts as follows:

$$\begin{cases} u = u_l + u_p \\ v = v_l + v_p \end{cases} \tag{9}$$

in which, the linear part, owing to corner node translations, can be expressed as:

$$\begin{cases} u_l = \alpha_1 + \alpha_2 x + \alpha_3 y \\ v_l = \alpha_4 + \alpha_5 x + \alpha_6 y \end{cases} \tag{10}$$

On the other hand, the higher-order displacement owing to the mid-side normal displacement DOFs can be written in a general form as:

$$U_p = \beta_1 + \beta_2 x + \beta_3 y + \beta_4 x^2 + \beta_5 xy + \beta_6 y^2 \tag{11}$$

This higher-order displacement field is because of the three mid-side node normal displacement *DOFs* (P_k). Therefore, it can be split into three parts – d_{p4}, d_{p5} and d_{p6} – where each part represents a displacement field owing to the contribution of one of the three mid-side node normal displacements P_4, P_5 and P_6, respectively. Then:

$$U_P = d_{P4} + d_{P5} + d_{P6} \tag{12}$$

These higher-order displacements d_{p4}, d_{p5} and d_{p6} due to mid-side node normal displacements P_4, P_5 and P_6 can be expressed as:

$$\begin{cases} d_{P4} = \left(a_1 + a_2 x + a_3 y + a_4 x^2 + a_5 xy + a_6 y^2\right) P_4 \\ d_{P5} = \left(b_1 + b_2 x + b_3 y + b_4 x^2 + b_5 xy + b_6 y^2\right) P_5 \\ d_{P6} = \left(d_1 + d_2 x + d_3 y + d_4 x^2 + d_5 xy + d_6 y^2\right) P_6 \end{cases} \tag{13}$$

The unknown constants (a_i, b_i, and d_i; for $i = 1 \ldots 6$) depend only on the element's geometry. Thus, they can be evaluated by exploiting the nodal boundary conditions. For this purpose, let us consider the displacement due to the mid-side node normal displacement P_4 of the edge (*1-2*). According to the standards of interpolation, the displacement d_{P4} due to the mid-side node normal displacement *DOF* (P_4) must be equal to P_4 at the node ($K = 4$) located at the edge (*1-2*) and zero at the other nodes, then we can write:

$$\begin{cases} a_1 + a_2x_1 + a_3y_1 + a_4x_1^2 + a_5x_1y_1 + a_6y_1^2 = 0 \\ a_1 + a_2x_4 + a_3y_4 + a_4x_4^2 + a_5x_4y_4 + a_6y_4^2 = 1 \\ a_1 + a_2x_2 + a_3y_2 + a_4x_2^2 + a_5x_2y_2 + a_6y_2^2 = 0 \\ a_1 + a_2x_5 + a_3y_5 + a_4x_5^2 + a_5x_5y_5 + a_6y_5^2 = 0 \\ a_1 + a_2x_3 + a_3y_3 + a_4x_3^2 + a_5x_3y_3 + a_6y_3^2 = 0 \\ a_1 + a_2x_6 + a_3y_6 + a_4x_6^2 + a_5x_6y_6 + a_6y_6^2 = 0 \end{cases} \tag{14}$$

with x_i and y_i are the *LST*'s nodal coordinates. If we adopt the reference system of Figure 1, then x_i and y_i will be: $x_1 = 0$; $x_4 = \frac{x_2}{2}$; $x_5 = \frac{x_2 + x_3}{2}$; $x_6 = \frac{x_3}{2}$; $y_1 = 0$; $y_2 = 0$; $y_4 = \frac{y_2}{2}$; $y_5 = \frac{y_2 + y_3}{2}$; $y_6 = \frac{y_3}{2}$.

After substituting (x_i, y_i; for $i = 1 \ldots 6$) in the system of equation (14), we get:

$$\begin{cases} a_1 = 0 \\ \frac{1}{4}a_4x_2^2 + \frac{1}{2}a_2x_2 + a_1 = 1 \\ a_4x_2^2 + a_2x_2 + a_1 = 0 \\ a_1 + \frac{1}{4}a_6y_3^2 + a_2\left(\frac{1}{2}x_2 + \frac{1}{2}x_3\right) + \frac{1}{2}a_3y_3 + a_4\left(\frac{1}{2}x_2 + \frac{1}{2}x_3\right)^2 + \frac{1}{2}a_5y_3\left(\frac{1}{2}x_2 + \frac{1}{2}x_3\right) = 0 \\ a_4x_3^2 + a_5x_3y_3 + a_2x_3 + a_6y_3^2 + a_3y_3 + a_1 = 0 \\ \frac{1}{4}a_4x_3^2 + \frac{1}{4}a_5x_3y_3 + \frac{1}{2}a_2x_3 + \frac{1}{4}a_6y_3^2 + \frac{1}{2}a_3y_3 + a_1 = 0 \end{cases} \tag{15}$$

The solution of the above system of equations provides:

$$a_1 = 0; \quad a_2 = \frac{4}{x_2}; \quad a_3 = -\frac{4x_3}{x_2y_3}; \quad a_4 = -\frac{4}{x_2^2}; \quad a_5 = -\frac{(4x_2 - 8x_3)}{x_2^2y_3};$$

$$a_6 = -\frac{(4x_3^2 - 4x_2x_3)}{x_2^2y_3^2}.$$

Let us now calculate the constants (b_i; for $i = 1 \ldots 6$) following the same practice. The displacement d_{P5} due to the *DOF* (P_5) must be equal to P_5 at the node ($K = 5$) located at the edge (*2-3*) and zero at the other nodes, then, we can write:

$$\begin{cases} b_1 + b_2x_1 + b_3y_1 + b_4x_1^2 + b_5x_1y_1 + b_6y_1^2 = 0 \\ b_1 + b_2x_4 + b_3y_4 + b_4x_4^2 + b_5x_4y_4 + b_6y_4^2 = 0 \\ b_1 + b_2x_2 + b_3y_2 + b_4x_2^2 + b_5x_2y_2 + b_6y_2^2 = 0 \\ b_1 + b_2x_5 + b_3y_5 + b_4x_5^2 + b_5x_5y_5 + b_6y_5^2 = 1 \\ b_1 + b_2x_3 + b_3y_3 + b_4x_3^2 + b_5x_3y_3 + b_6y_3^2 = 0 \\ b_1 + b_2x_6 + b_3y_6 + b_4x_6^2 + b_5x_6y_6 + b_6y_6^2 = 0 \end{cases} \tag{16}$$

After substituting (x_i, y_i; for $i = 1 \ldots 6$) in the system of equation (16), we get:

$$\begin{cases} b_1 = 0 \\ \frac{1}{4}\, b_4x_2^2 + \frac{1}{2}b_2x_2 + b_1 = 0 \\ b_4x_2^2 + b_2x_2 + b_1 = 0 \\ b_1 + \frac{1}{4}\, b_6y_3^2 + b_2\left(\frac{1}{2}\, x_2 + \frac{1}{2}x_3\right) + \frac{1}{2}\, b_3y_3 + b_4\left(\frac{1}{2}\, x_2 + \frac{1}{2}x_3\right)^2 + \frac{1}{2}b_5y_3\left(\frac{1}{2}\, x_2 + \frac{1}{2}x_3\right) = 1 \\ b_4x_3^2 + b_5x_3y_3 + b_2x_3 + b_6y_3^2 + b_3y_3 + b_1 = 0 \\ \frac{1}{4}\, b_4x_3^2 + \frac{1}{4}\, b_5x_3y_3 + \frac{1}{2}\, b_2x_3 + \frac{1}{4}\, b_6y_3^2 + \frac{1}{2}b_3y_3 + b_1 = 0 \end{cases} \tag{17}$$

The solution of the above system provides:

$$b_1 = 0; b_2 = 0; b_3 = 0; b_4 = 0; b_5 = \frac{4}{x_2y_3}; b_6 = -\frac{4x_3}{x_2y_3^2}.$$

Using the same practice, the displacement d_{P6} due to the *DOF* (P_6) must be equal to P_6 at the node ($K = 6$) located at the edge ($3 - 1$) and zero at the other nodes, then we can write:

$$\begin{cases} d_1 + d_2x_1 + d_3y_1 + d_4x_1^2 + d_5x_1y_1 + d_6y_1^2 = 0 \\ d_1 + d_2x_4 + d_3y_4 + d_4x_4^2 + d_5x_4y_4 + d_6y_4^2 = 0 \\ d_1 + d_2x_2 + d_3y_2 + d_4x_2^2 + d_5x_2y_2 + d_6y_2^2 = 0 \\ d_1 + d_2x_5 + d_3y_5 + d_4x_5^2 + d_5x_5y_5 + d_6y_5^2 = 0 \\ d_1 + d_2x_3 + d_3y_3 + d_4x_3^2 + d_5x_3y_3 + d_6y_3^2 = 0 \\ d_1 + d_2x_6 + d_3y_6 + d_4x_6^2 + d_5x_6y_6 + d_6y_6^2 = 1 \end{cases} \tag{18}$$

After substituting (x_i, y_i; for $i = 1 \ldots 6$) in the system of equation (18), we get:

$$\begin{cases} d_1 = 0 \\ \frac{1}{4}\, d_4x_2^2 + \frac{1}{2}d_2x_2 + d_1 = 0 \\ d_4x_2^2 + d_2x_2 + d_1 = 0 \\ d_1 + \frac{1}{4}\, d_6y_3^2 + d_2\left(\frac{1}{2}\, x_2 + \frac{1}{2}x_3\right) + \frac{1}{2}\, d_3y_3 + d_4\left(\frac{1}{2}\, x_2 + \frac{1}{2}x_3\right)^2 + \frac{1}{2}d_5y_3\left(\frac{1}{2}\, x_2 + \frac{1}{2}x_3\right) = 0 \\ d_4x_3^2 + d_5x_3y_3 + d_2x_3 + d_6y_3^2 + d_3y_3 + d_1 = 0 \\ \frac{1}{4}\, d_4x_3^2 + \frac{1}{4}\, d_5x_3y_3 + \frac{1}{2}\, d_2x_3 + \frac{1}{4}\, d_6y_3^2 + \frac{1}{2}d_3y_3 + d_1 = 1 \end{cases} \tag{19}$$

The solution of the above system provides:

$$d_1 = 0; d_2 = 0; d_3 = \frac{4}{y_3}; d_4 = 0; d_5 = -\frac{4}{x_2 y_3}; d_6 = -\frac{(4x_2 - 4x_3)}{x_2 y_3^2}.$$

Now, after having evaluated the constants – a_i, b_i, and d_i – let us express the higher-order displacement of equation (13) within the Cartesian system ($x - y$). The transformation between the systems ($n - t$) and ($x - y$) provides:

$$\begin{cases} u_{p4} = d_{p4} \cdot C_{12} \\ v_{p4} = d_{p4} \cdot S_{12} \end{cases}, \begin{cases} u_{p5} = d_{p5} \cdot C_{23} \\ v_{p5} = d_{p5} \cdot S_{23} \end{cases}, \text{ and } \begin{cases} u_{p6} = d_{p6} \cdot C_{31} \\ v_{p6} = d_{p6} \cdot S_{31} \end{cases} \tag{20}$$

By substituting (equations 20, 13, 10) into equation (9), we get the following in-plane displacement field:

$$\begin{cases} u = \alpha_1 + \alpha_2 x + \alpha_3 y + (a_1 + a_2 x + a_3 y + a_4 x^2 + a_5 xy + a_6 y^2) C_{12} \cdot P_4 \\ \quad + (b_1 + b_2 x + b_3 y + b_4 x^2 + b_5 xy + b_6 y^2) C_{23} \cdot P_5 + (d_1 + d_2 x + d_3 y + d_4 x^2 + d_5 xy + d_6 y^2) C_{31} \cdot P_6 \\ v = \alpha_4 + \alpha_5 x + \alpha_6 y + (a_1 + a_2 x + a_3 y + a_4 x^2 + a_5 xy + a_6 y^2) S_{12} \cdot P_4 \\ \quad + (b_1 + b_2 x + b_3 y + b_4 x^2 + b_5 xy + b_6 y^2) S_{23} \cdot P_5 + (d_1 + d_2 x + d_3 y + d_4 x^2 + d_5 xy + d_6 y^2) S_{31} \cdot P_6 \end{cases} \tag{21}$$

In the above expression, we have calculated all the constants a_i, b_i, and d_i, then, we left with nine unknowns only, which are the six interpolation's coefficients – α_1, α_2, α_3, α_4, α_5, α_6 – and the three mid-side normal displacements: P_4, P_5, P_6. Note that the three mid-side normal displacements P_4, P_5 and P_6 are unknown, and we aim to express them in terms of nodal drilling rotational quantities, so, they can be considered as unknown parameters of the polynomial interpolation by assuming: $P_4 = \alpha_7$, $P_5 = \alpha_8$ and $P_6 = \alpha_9$.

Finally, the displacement field of equation (8) is now expressed in terms of nine unknown parameters as follows:

$$\begin{cases} u = \alpha_1 + \alpha_2 x + \alpha_3 y + (a_1 + a_2 x + a_3 y + a_4 x^2 + a_5 xy + a_6 y^2) C_{12} \cdot \alpha_7 \\ + (b_1 + b_2 x + b_3 y + b_4 x^2 + b_5 xy + b_6 y^2) C_{23} \cdot \alpha_8 + (d_1 + d_2 x + d_3 y + d_4 x^2 + d_5 xy + d_6 y^2) C_{31} \cdot \alpha_9 \\ v = \alpha_4 + \alpha_5 x + \alpha_6 y + (a_1 + a_2 x + a_3 y + a_4 x^2 + a_5 xy + a_6 y^2) S_{12} \cdot \alpha_7 \\ + (b_1 + b_2 x + b_3 y + b_4 x^2 + b_5 xy + b_6 y^2) S_{23} \cdot \alpha_8 + (d_1 + d_2 x + d_3 y + d_4 x^2 + d_5 xy + d_6 y^2) S_{31} \cdot \alpha_9 \end{cases} \tag{22}$$

According to continuum mechanics, the true drilling rotational field is obtained by substituting equation (22) in equation (7), as:

$$\begin{aligned} \varphi = & -\frac{1}{2}\alpha_3 + \frac{1}{2}\alpha_5 - \left(\frac{1}{2} C_{12} a_3 - \frac{1}{2} S_{12} a_2 + \frac{1}{2} x C_{12} a_5 + y C_{12} a_6 - x S_{12} a_4 - \frac{1}{2} y S_{12} a_5\right) \alpha_7 \\ & - \left(\frac{1}{2} C_{23} b_3 - \frac{1}{2} S_{23} b_2 + \frac{1}{2} x C_{23} b_5 + y C_{23} b_6 - x S_{23} b_4 - \frac{1}{2} y S_{23} b_5\right) \alpha_8 \\ & - \left(\frac{1}{2} C_{31} d_3 - \frac{1}{2} S_{31} d_2 + \frac{1}{2} x C_{31} d_5 + y C_{31} d_6 - x S_{31} d_4 - \frac{1}{2} y S_{31} d_5\right) \alpha_9 \end{aligned} \tag{23}$$

There are several constants among a_i, b_i, and d_i with a null value. After substitution, we get a simpler form of the displacement and rotation interpolations as follows:

$$\begin{cases} u = \alpha_1 + \alpha_2 x + \alpha_3 y + \alpha_7 C_{12}\left(a_2 x + a_3 y + a_4 x^2 + a_5 xy + a_6 y^2\right) + \alpha_8 C_{23}\left(b_5 xy + b_6 y^2\right) + \alpha_9 C_{31}\left(d_3 y + d_5 xy + d_6 y^2\right) \\ v = \alpha_4 + \alpha_5 x + \alpha_6 y + \alpha_7 S_{12}\left(a_2 x + a_3 y + a_4 x^2 + a_5 xy + a_6 y^2\right) + \alpha_8 S_{23}\left(b_5 xy + b_6 y^2\right) + \alpha_9 S_{31}\left(d_3 y + d_5 xy + d_6 y^2\right) \\ \varphi = -\frac{1}{2}\alpha_3 + \frac{1}{2}\alpha_5 + \left(\frac{1}{2} S_{12} a_2 - \frac{1}{2} C_{12} a_3 - \frac{1}{2} x C_{12} a_5 - y C_{12} a_6 + x S_{12} a_4 + \frac{1}{2} y S_{12} a_5\right)\alpha_7 + \\ \quad + \left(\frac{1}{2} y S_{23} b_5 - y C_{23} b_6 - \frac{1}{2} x C_{23} b_5\right)\alpha_8 + \left(\frac{1}{2} y S_{31} d_5 - \frac{1}{2} x C_{31} d_5 - y C_{31} d_6 - \frac{1}{2} C_{31} d_3\right)\alpha_9 \end{cases} \tag{24}$$

In matrix form:

$$\begin{Bmatrix} u \\ v \\ \varphi \end{Bmatrix} = \begin{bmatrix} 1 & x & y & 0 & 0 & 0 & C_{12}\left(a_2 x + a_3 y + a_4 x^2 + a_5 xy + a_6 y^2\right) & C_{23}\left(b_5 xy + b_6 y^2\right) & C_{31}\left(d_3 y + d_5 xy + d_6 y^2\right) \\ 0 & 0 & 0 & 1 & x & y & S_{12}\left(a_2 x + a_3 y + a_4 x^2 + a_5 xy + a_6 y^2\right) & S_{23}\left(b_5 xy + b_6 y^2\right) & S_{31}\left(d_3 y + d_5 xy + d_6 y^2\right) \\ 0 & 0 & -\frac{1}{2} & 0 & \frac{1}{2} & 0 & \frac{1}{2} S_{12} a_2 - \frac{1}{2} C_{12} a_3 - \frac{1}{2} x C_{12} a_5 - y C_{12} a_6 + x S_{12} a_4 + \frac{1}{2} y S_{12} a_5 & \frac{1}{2} y S_{23} b_5 - y C_{23} b_6 - \frac{1}{2} x C_{23} b_5 & \frac{1}{2} y S_{31} d_5 - \frac{1}{2} x C_{31} d_5 - y C_{31} d_6 - \frac{1}{2} C_{31} d_3 \end{bmatrix} \begin{Bmatrix} \alpha_1 \\ \vdots \\ \alpha_9 \end{Bmatrix} \tag{25}$$

Based on the linear strain-displacement relationship, strain vector is defined as:

$$\begin{cases} \varepsilon_x = \dfrac{\partial u}{\partial x} = \alpha_2 + (a_2 + 2x a_4 + y a_5) C_{12} \cdot \alpha_7 + y b_5 C_{23} \alpha_8 + y d_5 C_{31} \alpha_9 \\ \varepsilon_y = \dfrac{\partial v}{\partial y} = \alpha_6 + (a_3 + x a_5 + 2y a_6) S_{12} \cdot \alpha_7 + (x b_5 + 2y b_6) S_{23} \cdot \alpha_8 + (d_3 + x d_5 + 2y d_6) S_{31} \cdot \alpha_9 \\ \gamma_{xy} = \left(\dfrac{\partial u}{\partial y} + \dfrac{\partial v}{\partial x}\right) = \alpha_3 + \alpha_5 + (C_{12} a_3 + S_{12} a_2 + x C_{12} a_5 + 2y C_{12} a_6 + 2x S_{12} a_4 + y S_{12} a_5)\alpha_7 \\ \qquad\qquad + (x C_{23} b_5 + 2y C_{23} b_6 + y S_{23} b_5)\alpha_8 + (C_{31} d_3 + x C_{31} d_5 + 2y C_{31} d_6 + y S_{31} d_5)\alpha_9 \end{cases} \tag{26}$$

The strain matrix $[B]$ is then:

$$[B] = \begin{bmatrix} 0 & 1 & 0 & 0 & 0 & 0 & C_{12} a_2 + 2 C_{12} a_4 x + C_{12} a_5 y & C_{21} b_5 y & C_{31} d_5 y \\ 0 & 0 & 0 & 0 & 0 & 1 & S_{12} a_3 + S_{12} a_5 x + 2 S_{12} a_6 y & S_{21} b_5 x + 2 S_{21} b_6 y & S_{31} d_3 + S_{31} d_5 x + 2 S_{31} d_6 y \\ 0 & 0 & 1 & 0 & 1 & 0 & C_{12} a_3 + S_{12} a_2 + C_{12} a_5 x + 2 C_{12} a_6 y + 2 S_{12} a_4 x + S_{12} a_5 y & C_{21} b_5 x + 2 C_{21} b_6 y + S_{21} b_5 y & C_{31} d_3 + C_{31} d_5 x + 2 C_{31} d_6 y + S_{31} d_5 y \end{bmatrix} \begin{Bmatrix} \alpha_1 \\ \vdots \\ \alpha_9 \end{Bmatrix} \tag{27}$$

3.3 Incorporating the true drilling rotational degree of freedom

After calculating the displacement fields, the nine unknown parameters (α_i; for $i = 1 \ldots 9$) of the polynomial interpolation can be now expressed in terms of the nine nodal DOFs (u_i, v_i,

φ_i; for $i = 1 \ldots 3$) of the three-nodded triangular element via the transformation matrix $[A]$. By means of this transformation, we can incorporate the nodal rotations in the expression of the displacement field by applying:

$$\{U\} = [A]\{\alpha\} \tag{28}$$

The transformation matrix $[A]$ is calculated by substituting the coordinates (x_i, y_i; for $i = 1 \ldots 3$) of each node ($i = 1, 2, 3$) into the displacement variables (u, v and φ). The transformation matrix $[A]$ may be partitioned into the following form:

$$[A] = \begin{bmatrix} A_1 \\ A_2 \\ A_3 \end{bmatrix} \tag{29}$$

The 3×9 matrices $[A_i]$ are given as:

$$[A_i] = \begin{bmatrix} 1 & x_i & y_i & 0 & 0 & 0 & 0 & 0 & 0 \\ 0 & 0 & 0 & 1 & x_i & y_i & 0 & 0 & 0 \\ 0 & 0 & -\frac{1}{2} & 0 & \frac{1}{2} & 0 & \frac{1}{2}S_{12}a_2 - \frac{1}{2}C_{12}a_3 - \frac{1}{2}C_{12}a_5x_i - C_{12}a_6y_i + S_{12}a_4x_i + \frac{1}{2}S_{12}a_5y_i & \frac{1}{2}S_{23}b_3y_i - C_{23}b_6y_i - \frac{1}{2}C_{23}b_5x_i & \frac{1}{2}S_{31}d_3y_i - \frac{1}{2}C_{31}d_5x_i - C_{31}d_6y_i - \frac{1}{2}C_{31}d_3 \end{bmatrix} \tag{30}$$

Note that when we have evaluated the constants a_i, b_i and d_i, we have chosen the reference system of Figure 1. Therefore, we have considered: $x_1 = 0$; $y_1 = 0$; $y_2 = 0$; $C_{12} = 0$; $S_{12} = -1$. By substituting these values and the values of the constants a_i, b_i, and d_i, and by considering $C_{ij} = \frac{(y_j - y_i)}{l_{ij}}$, $S_{ij} = \frac{-(x_j - x_i)}{l_{ij}}$ and $l_{12} = x_2$, we get the simplest form of the transformation matrix $[A]$ as:

$$[A] = \begin{bmatrix} 1 & 0 & 0 & 0 & 0 & 0 & 0 & 0 & 0 \\ 0 & 0 & 0 & 1 & 0 & 0 & 0 & 0 & 0 \\ 0 & 0 & -\frac{1}{2} & 0 & \frac{1}{2} & 0 & -\frac{2}{l_{12}} & 0 & \frac{2}{l_{31}} \\ 1 & x_2 & 0 & 0 & 0 & 0 & 0 & 0 & 0 \\ 0 & 0 & 0 & 1 & x_2 & 0 & 0 & 0 & 0 \\ 0 & 0 & -\frac{1}{2} & 0 & \frac{1}{2} & 0 & \frac{2}{l_{12}} & -\frac{2}{l_{23}} & 0 \\ 1 & x_3 & y_3 & 0 & 0 & 0 & 0 & 0 & 0 \\ 0 & 0 & 0 & 1 & x_3 & y_3 & 0 & 0 & 0 \\ 0 & 0 & -\frac{1}{2} & 0 & \frac{1}{2} & 0 & 0 & \frac{2}{l_{23}} & -\frac{2}{l_{31}} \end{bmatrix} \tag{31}$$

As a result, the obtained transformation matrix $[A]$ provides the following expressions for the true nodal drilling rotations:

$$\begin{cases} \varphi_1 = -\dfrac{1}{2}\,\alpha_3 + \dfrac{1}{2}\alpha_5 - \dfrac{2}{l_{12}}\alpha_7 + \dfrac{2}{l_{31}}\alpha_9 \\ \varphi_2 = -\dfrac{1}{2}\,\alpha_3 + \dfrac{1}{2}\alpha_5 + \dfrac{2}{l_{12}}\alpha_7 - \dfrac{2}{l_{23}}\alpha_8 \\ \varphi_3 = -\dfrac{1}{2}\,\alpha_3 + \dfrac{1}{2}\alpha_5 + \dfrac{2}{l_{23}}\alpha_8 - \dfrac{2}{l_{31}}\alpha_9 \end{cases} \tag{32}$$

bearing in mind that α_7, α_8 and α_9 are the mid-side normal displacement P_4, P_5 and P_6, respectively.

As we have split the displacement field in equations (9) and (10) into linear and higher-order parts u_l and u_p, respectively, the nodal rotations can also be split following the same practice into: $\varphi_i = \varphi_l + \varphi_P$.where:

φ_l, is the rotation due to the linear displacement: $\varphi_l = -\frac{1}{2}\,\alpha_3 + \frac{1}{2}\alpha_5$.

φ_P, is the rotation due to the higher order displacement, it is expressed in terms of α_7, α_8 and α_9.

It can be seen that φ_l is constant over the whole element, which implies that φ_l represents the rigid body rotation Φ_R of the developed element.

In addition, it is clear that: $\varphi_l = \phi_R = \frac{\varphi_1 + \varphi_2 + \varphi_3}{3} = -\frac{1}{2}\,\alpha_3 + \frac{1}{2}\alpha_5$.

So, we have: $\varphi_i = \phi_R + \varphi_P$

We can also easily notice that: $\varphi_{P1} + \varphi_{P2} + \varphi_{P3} = 0$.

Furthermore, by considering: $P_4 = \alpha_7$, $P_5 = \alpha_8$ and $P_6 = \alpha_9$, we obtain:

$$\begin{cases} (\varphi_2 - \varphi_1) = \dfrac{4}{l_{12}}P_4 - \dfrac{2}{l_{23}}P_5 - \dfrac{2}{l_{31}}P_6 \\ (\varphi_3 - \varphi_2) = \dfrac{4}{l_{23}}P_5 - \dfrac{2}{l_{31}}P_6 - \dfrac{2}{l_{12}}P_4 \\ (\varphi_1 - \varphi_3) = \dfrac{4}{l_{31}}P_6 - \dfrac{2}{l_{12}}P_4 - \dfrac{2}{l_{23}}P_5 \end{cases} \tag{33}$$

These expressions are obviously different from those of the transformation used for Allman's interpolation: $(\omega_j - \omega_i) = \frac{8}{l_{ij}}P_k$; for $i = 1, 2, 3$; $j = 3, 1, 2$; and $k = 4, 5, 6$.

Equation (33), shows that the resulted displacement field is incompatible because, to satisfy the inter-element continuity, the mid-side displacement P_k must be defined along the element's edge (ij) by the rotations of the nodes associated with that edge (ij) only.

As a final comment, it is easy to notice that the central rotation:

$$\phi_0(x_0, y_0) = \frac{\varphi_1 + \varphi_2 + \varphi_3}{3} = \phi_R = -\frac{1}{2}\,\alpha_3 + \frac{1}{2}\alpha_5.$$

with:

$$x_0 = \frac{x_1 + x_2 + x_3}{3};\; y_0 = \frac{y_1 + y_2 + y_3}{3}$$

.

3.4 The transformation matrix

After calculating the transformation matrix, the element stiffness matrix can be calculated following the well-known procedure for displacement type finite elements, using the following general expression:

$$[K] = [A^{-1}]^T \left(\int_v [B]^T [D][B] dv \right) [A^{-1}] \tag{34}$$

With $[A]$ have to be a non-singular matrix.

However, the obtained transformation matrix $[A]$ of the developed element is singular because the sum of the drilling rotations due to the higher-order displacements α_7, α_8 and α_9 is null. In this case, one of the three equations that express (α_7, α_8 and α_9) in terms of (φ_1, φ_2 and φ_3) in the matrix $[A]$ is trivial, and it provides no additional information to the system of equations, which leads to a singular transformation matrix. In other words, the third, sixth and ninth rows of matrix $[A]$ are linearly dependent. This means that we have a missing equation because it can be expressed by the two others.

If we analyse the system of equation (31), we can easily notice that the system implies no restriction on the mid-side node *DOFs* (α_7, α_8, and α_9). If we inspect the simple case when: $\varphi_1 = \varphi_2 = \varphi_3 = 0$. We can easily notice that this configuration is not only fulfilled when $\alpha_7 = \alpha_8 = \alpha_9 = 0$ but, there exist also an infinity of (α_7, α_8 and α_9) that fulfils this condition. According to equation (32), the configuration: $\varphi_1 = \varphi_2 = \varphi_3 = \varphi_R$, with φ_R can be a zero or any non-zero value of rigid rotation, will be satisfied whenever: $\frac{1}{l_{12}}\alpha_7 = \frac{1}{l_{23}}\alpha_8 = \frac{1}{l_{31}}\alpha_9$, even for non-zero values of (α_7, α_8, and α_9). Which implies that the condition $\frac{1}{l_{12}}\alpha_7 = \frac{1}{l_{23}}\alpha_8 = \frac{1}{l_{31}}\alpha_9$ gives the kernel of the transformation matrix $[A]$.

Consequently, the singularity of the system of the transformation matrix $[A]$ arises from the fact that there is an infinity of (α_7, α_8, and α_9) that fulfils one configuration that corresponds to: $\varphi_{p1} = \varphi_{p2} = \varphi_{p3} = 0$.

If we schematically interpret the nodal drilling rotational *DOFs* as the vertex bisecting the angle between two adjacent edges of the element (the average rotations of the element corner edges), then, Figure 3 (a), (b) and (c) shows the existence of infinity of solutions.

It is clear that these configurations can be reached only by manipulating the normal displacements of the mid-side nodes. Thus, these configurations are not allowed here because the mid-side nodes are eliminated and the corresponding displacement is related to corner rotations.

To overcome this obstacle, the configurations shown in Figure 3 (b) and (c) have to be restricted to make $\varphi_1 = \varphi_2 = \varphi_3$ or equivalently $\varphi_{p1} = \varphi_{p2} = \varphi_{p3} = 0$ can occur only when $\alpha_7 = \alpha_8 = \alpha_9 = 0$. In other words, the set $\frac{2}{l_{12}}\alpha_7 = \frac{2}{l_{23}}\alpha_8 = \frac{2}{l_{31}}\alpha_9$ must be prohibited. This means that we need to impose an additional constraint on the (α_7, α_8 and α_9) kinematic. Practically we can arrange this difficulty by adding an additional equation to the system of equation (31) to overcome the singularity of the transformation matrix. Hence, the corner nodes rotational *DOFs* are amended with an additional equation that embodies the required constraint condition.

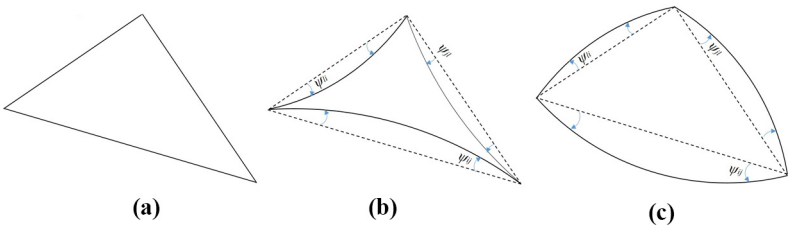

Figure 3.
Several configurations with zero nodal drilling rotations

Of course, the additional equation to be added to the corner node rotations in equation (31) must be a neuter equation, so if we add a zero quantity to the rotational *DOFs*, we expect that the considered rotational *DOFs* will still represent the true drilling rotations.

In this purpose, the penalty method is adopted here to well impose the required kinematic condition onto the solution of the system of equation (32). Accordingly, the rotational *DOFs* of the transformation matrix $[A]$ will be amended by the quantity:

$$k(D\alpha_7 + E\alpha_8 + F\alpha_9) \tag{35}$$

The above quantity is the general form of any amendment, and it is supposed to be null, which means:

$$D\alpha_7 + E\alpha_8 + F\alpha_9 = 0 \tag{36}$$

It is obvious that the solution of this problem implies a geometric relation between the three mid-side nodes normal displacement α_7, α_8 and α_9.

Then, the transformation matrix $[A]$ becomes:

$$[A] = \begin{bmatrix} 1 & 0 & 0 & 0 & 0 & 0 & 0 & 0 & 0 \\ 0 & 0 & 0 & 1 & 0 & 0 & 0 & 0 & 0 \\ 0 & 0 & -\frac{1}{2} & 0 & \frac{1}{2} & 0 & k\cdot D - \frac{2}{l_{12}} & k\cdot E & k\cdot F + \frac{2}{l_{31}} \\ 1 & x_2 & 0 & 0 & 0 & 0 & 0 & 0 & 0 \\ 0 & 0 & 0 & 1 & x_2 & 0 & 0 & 0 & 0 \\ 0 & 0 & -\frac{1}{2} & 0 & \frac{1}{2} & 0 & k\cdot D + \frac{2}{l_{12}} & k\cdot E - \frac{2}{l_{23}} & k\cdot F \\ 1 & x_3 & y_3 & 0 & 0 & 0 & 0 & 0 & 0 \\ 0 & 0 & 0 & 1 & x_3 & y_3 & 0 & 0 & 0 \\ 0 & 0 & -\frac{1}{2} & 0 & \frac{1}{2} & 0 & k\cdot D & k\cdot E + \frac{2}{l_{23}} & k\cdot F - \frac{2}{l_{31}} \end{bmatrix} \tag{37}$$

where k is a constant with a relatively large magnitude.

It is important here, in the aim to get an invariant element, to add the quantity in equation (35) to the expressions of φ_1, φ_2 and φ_3 transformations, which are the third, the sixth and the ninth rows in the transformation matrix $[A]$, respectively. It is also important to choose the constant k bigger enough than the $max(A_{ij})$. By this way, the formulated finite element is invariant, nevertheless, it implies an adjustable constant k.

Hence, the inverse of the transformation matrix $[A]$ in equation (37), will be the following:

$$[H] = [A]^{-1} = \begin{bmatrix} 1 & 0 & 0 & 0 & 0 & 0 & 0 & 0 & 0 \\ -\frac{1}{x_2} & 0 & 0 & \frac{1}{x_2} & 0 & 0 & 0 & 0 & 0 \\ -\frac{(x_2 - x_3)}{x_2 y_3} & 0 & 0 & -\frac{x_3}{x_2 y_3} & 0 & 0 & \frac{1}{y_3} & 0 & 0 \\ 0 & 1 & 0 & 0 & 0 & 0 & 0 & 0 & 0 \\ 0 & -\frac{1}{x_2} & 0 & 0 & \frac{1}{x_2} & 0 & 0 & 0 & 0 \\ 0 & -\frac{(x_2 - x_3)}{x_2 y_3} & 0 & 0 & -\frac{x_3}{x_2 y_3} & 0 & 0 & \frac{1}{y_3} & 0 \\ H_{71} & H_{72} & H_{73} & H_{74} & H_{75} & H_{76} & H_{77} & H_{78} & H_{79} \\ H_{81} & H_{82} & H_{83} & H_{84} & H_{85} & H_{86} & H_{87} & H_{88} & H_{89} \\ H_{91} & H_{92} & H_{93} & H_{94} & H_{95} & H_{96} & H_{97} & H_{98} & H_{99} \end{bmatrix} \quad (38)$$

where H_{ij} are given in Table A.I in Appendix 1 (for $i = 7 \ldots 9$ and $j = 1 \ldots 9$).

Note that, the imposed constraint $k(D\alpha_7 + E\alpha_8 + F\alpha_9) = 0$ via the penalty method will be well imposed as bigger is the constant k. For this purpose, if we set k to be very large compared to A_{ij} terms, then l_{ij}, x_{ij} and y_{ij} can be neglected in comparison to k, which yields:

$H_{71} = H_{81} = H_{91} = H_{72} = H_{82} = H_{92} = H_{74} = H_{84} = H_{94} = H_{75} = H_{85} = H_{95} = H_{76} = H_{87} = H_{97} = H_{78} = H_{88} = H_{98} = 0$.

Moreover, H_{73}, H_{76}, H_{79}, H_{83}, H_{86}, H_{89}, H_{93}, H_{96} and H_{99} will be as in Table A.II.

The interpolation's constants (α_i; for $i = 1 \ldots 9$), are given by: $\{\alpha\} = [H]\{U\}$, which provides:

$$\begin{cases} \alpha_7 = H_{73}\varphi_1 + H_{76}\varphi_2 + H_{79}\varphi_3 \\ \alpha_8 = H_{83}\varphi_1 + H_{86}\varphi_2 + H_{89}\varphi_3 \\ \alpha_9 = H_{93}\varphi_1 + H_{96}\varphi_2 + H_{99}\varphi_3 \end{cases} \quad (39)$$

This set of equations represents the general form of the solution. It is expressed in terms of D, E and F, and it satisfies equation (36). Which means that φ_i in the above equation represents the true drilling rotational *DOF*.

After substituting the values of the parameters: H_{73}, H_{76}, … H_{99} from Table A.II into equation (39), the solution of the above system in terms of D, E and F provides:

$$\begin{cases} D = \dfrac{E\, l_{23}}{l_{12}} \dfrac{\varphi_1 + \varphi_2 - 2\varphi_3}{\varphi_2 - 2\varphi_1 + \varphi_3} \\ F = \dfrac{E\, l_{23}}{l_{31}} \dfrac{\varphi_1 - 2\varphi_2 + \varphi_3}{\varphi_2 - 2\varphi_1 + \varphi_3} \end{cases} \quad (40)$$

However, this solution is trivial because it provides zero in the denominator of H_{ij} factors. Note that D, E and F are dependent because α_7, α_8 and α_9 are linearly dependent.

To get a non-trivial solution, let us consider the inter elements compatibility condition. According to Figure 1, the compatibility condition implies that a mid-side displacement P_k needs to be expressed only in terms of the two nodal rotations φ_i and φ_j pertinent to the same element's side (ij). The application of this requirement on equation (39), allows us to consider:

$$H_{79} = H_{83} = H_{96} = 0 \quad (41)$$

Then, we get the following system:

$$\begin{cases} Fl_{12}l_{31} - El_{12}l_{23} = 0 \\ Dl_{12}l_{23} - Fl_{23}l_{31} = 0 \\ El_{23}l_{31} - Dl_{12}l_{31} = 0 \end{cases} \tag{42}$$

Which yields:

$$\begin{cases} D = E\dfrac{l_{23}}{l_{12}} \\ F = E\dfrac{l_{23}}{l_{31}} \end{cases} \tag{43}$$

In addition, the constants D, E and F need to satisfy equation (36) in which E, D and F must have the same dimensions as those of α_i multipliers in (equations 31 and 32) then, we get:

$$\begin{cases} D = \dfrac{1}{l_{12}} \\ E = \dfrac{1}{l_{23}} \\ F = \dfrac{1}{l_{31}} \end{cases} \tag{44}$$

By substituting in equation (36), we obtain the following kinematic relation between mi-side normal displacements:

$$\frac{1}{l_{12}}\alpha_7 + \frac{1}{l_{23}}\alpha_8 + \frac{1}{l_{31}}\alpha_9 = 0 \tag{45}$$

The above relation is the kinematic constraint that we can apply to the mid-side normal displacements (α_7, α_8, and α_9) that satisfies the neutrality of equation (35) and the inter-element compatibility. Hence, this is the constraint that removes the transformation matrix $[A]$ singularity while preserving the exactitude and the correctness of the true drilling rotational *DOF*.

Note that equation (45), is equivalent to equation (6). Nevertheless, in our formulation, we did not apply any constraint on the rotational field, but what we did is that we have imposed a kinematic constraint on α_7, α_8 and α_9 to make: $k\left(\frac{1}{l_{12}}\alpha_7 + \frac{1}{l_{23}}\alpha_8 + \frac{1}{l_{31}}\alpha_9\right) = 0$. This constraint when applied will only restrain the possible configurations of (α_7, α_8 and α_9) to remove the transformation matrix singularity as we have explained in the aforementioned section.

Here again, the relation between mid-side normal displacements in equation (45) is because of the inter-elements compatibility condition when applied to the parabolic displacement field.

3.5 The element stiffness matrix

After having the correct constraint that must be added to the singular transformation matrix, the penalty method will be used to impose the kinematic condition of equation (45) onto the solution of the system of equation (31). Accordingly, the third, the sixth and the ninth rows of the transformation matrix will be amended by the quantity: $k\left(\frac{1}{l_{12}}\alpha_7+\frac{1}{l_{23}}\alpha_8+\frac{1}{l_{31}}\alpha_9\right)$.

Then, the transformation matrix $[A]$ of equation (31) becomes:

$$[A]=\begin{bmatrix}
1 & 0 & 0 & 0 & 0 & 0 & 0 & 0 & 0\\
0 & 0 & 0 & 1 & 0 & 0 & 0 & 0 & 0\\
0 & 0 & -\frac{1}{2} & 0 & \frac{1}{2} & 0 & \frac{1}{l_{12}}(k-2) & \frac{1}{l_{23}}k & \frac{1}{l_{31}}(k+2)\\
1 & x_2 & 0 & 0 & 0 & 0 & 0 & 0 & 0\\
0 & 0 & 0 & 1 & x_2 & 0 & 0 & 0 & 0\\
0 & 0 & -\frac{1}{2} & 0 & \frac{1}{2} & 0 & \frac{1}{l_{12}}(k+2) & \frac{1}{l_{23}}(k-2) & \frac{1}{l_{31}}k\\
1 & x_3 & y_3 & 0 & 0 & 0 & 0 & 0 & 0\\
0 & 0 & 0 & 1 & x_3 & y_3 & 0 & 0 & 0\\
0 & 0 & -\frac{1}{2} & 0 & \frac{1}{2} & 0 & \frac{1}{x_2}k & \frac{1}{l_{23}}(k+2) & \frac{1}{l_{31}}(k-2)
\end{bmatrix} \tag{46}$$

In this case, the inverse of the transformation matrix $[A]$ can be evaluated explicitly as:

$$[A]^{-1}=\begin{bmatrix}
1 & 0 & 0 & 0 & 0 & 0 & 0 & 0 & 0\\
-\frac{1}{x_2} & 0 & 0 & \frac{1}{x_2} & 0 & 0 & 0 & 0 & 0\\
-\frac{(x_2-x_3)}{x_2y_3} & 0 & 0 & -\frac{x_3}{x_2y_3} & 0 & 0 & \frac{1}{y_3} & 0 & 0\\
0 & 1 & 0 & 0 & 0 & 0 & 0 & 0 & 0\\
0 & -\frac{1}{x_2} & 0 & 0 & \frac{1}{x_2} & 0 & 0 & 0 & 0\\
0 & -\frac{(x_2-x_3)}{x_2y_3} & 0 & 0 & -\frac{x_3}{x_2y_3} & 0 & 0 & \frac{1}{y_3} & 0\\
-\frac{(x_2-x_3)}{6ky_3} & \frac{1}{6k} & \frac{(2x_2-3kx_2)}{18k} & -\frac{x_3}{6ky_3} & -\frac{1}{6k} & \frac{(2x_2+3kx_3)}{18k} & \frac{x_2}{6ky_3} & 0 & \frac{x_2}{9k}\\
-\frac{l_{23}(x_2-x_3)}{6kx_2y_3} & \frac{l_{23}}{6kx_2} & \frac{l_{23}}{9k} & -\frac{l_{23}x_3}{6kx_2y_3} & -\frac{l_{23}}{6kx_2} & \frac{(2l_{23}-3kl_{23})}{18k} & \frac{l_{23}}{6ky_3} & 0 & \frac{(2l_{23}+3kl_{23})}{18k}\\
-\frac{l_{31}(x_2-x_3)}{6kx_2y_3} & \frac{l_{31}}{6kx_2} & \frac{(2l_{31}+3kl_{31})}{18k} & -\frac{l_{31}x_3}{6kx_2y_3} & -\frac{l_{31}}{6kx_2} & \frac{l_{31}}{9k} & \frac{l_{31}}{6ky_3} & 0 & \frac{(2l_{23}-3kl_{23})}{18k}
\end{bmatrix} \tag{47}$$

As we have mentioned previously, if we set k to be large enough, then l_{ij}, x_{ij} and y_{ij} can be neglected in comparison to k, which yields:

$$[H] = [A]^{-1} = \begin{bmatrix} 1 & 0 & 0 & 0 & 0 & 0 & 0 & 0 & 0 \\ -\frac{1}{x_2} & 0 & 0 & \frac{1}{x_2} & 0 & 0 & 0 & 0 & 0 \\ -\frac{(x_2 - x_3)}{x_2 y_3} & 0 & 0 & -\frac{x_3}{x_2 y_3} & 0 & 0 & \frac{1}{y_3} & 0 & 0 \\ 0 & 1 & 0 & 0 & 0 & 0 & 0 & 0 & 0 \\ 0 & -\frac{1}{x_2} & 0 & 0 & \frac{1}{x_2} & 0 & 0 & 0 & 0 \\ 0 & -\frac{(x_2 - x_3)}{x_2 y_3} & 0 & 0 & -\frac{x_3}{x_2 y_3} & 0 & 0 & \frac{1}{y_3} & 0 \\ 0 & 0 & \frac{-l_{12}}{6} & 0 & 0 & \frac{l_{12}}{6} & 0 & 0 & 0 \\ 0 & 0 & 0 & 0 & 0 & -\frac{l_{23}}{6} & 0 & 0 & \frac{l_{23}}{6} \\ 0 & 0 & \frac{l_{31}}{6} & 0 & 0 & 0 & 0 & 0 & -\frac{l_{31}}{6} \end{bmatrix} \tag{48}$$

Then, the element stiffness matrix is calculated using the following expression:

$$[K] = [H]^T \left(\int_v [B]^T [D][B] dv \right) [H] \tag{49}$$

It is worthy to note that the above expression is independent of any numerical adjustable parameter because in equation (48) the numerical constant k does not appear in the stiffness matrix formulation.

4. Inspect the validity of assumptions

It is important here to illustrate the importance of having the explicit expression of $[H]$ matrix. In addition to the reduced numerical cost, the matrix $[H]$ allows the possibility of expressing the displacement and the rotational fields explicitly in terms of nodal DOFs. By substituting $\{\alpha\} = [H]\{U\}$ into equation (25), we obtained the explicit expressions of the displacement and rotational fields presented in Appendix 2.

As we have assumed in equations (9-13), it is found that the linear displacement is expressed in terms of the nodal translations, while the higher order is governed by the nodal rotations. The drilling rotational field is a linear function expressed as:

$$\varphi(x,y) = \varphi_R + N_1(x,y)\varphi_{P1} + N_2(x,y)\varphi_{P2} + N_3(x,y)\varphi_{P3} \tag{50}$$

Moreover, according to equation (48) the present formulation provides the following expression of the mid-side normal displacement in terms of nodal true drilling rotations:

$$\alpha_k = \frac{l_{ij}}{6}(\varphi_j - \varphi_i) \tag{51}$$

with: $k = 7, 8, 9$ when $i = 2, 3, 1$ and $j = 1, 2, 3$.

Most importantly, the matrix $[H]$ allows the possibility of investigating the effect of the constraints we have imposed to the solution of the transformation matrix of the system of equation (31), especially on the correctness of the true physical interpretation of the drilling rotational *DOF*. According to the constrained matrix $[A]$ of equation (37), the nodal rotations are:

$$\begin{cases} \varphi_1 = -\frac{1}{2}\alpha_3 + \frac{1}{2}\alpha_5 + \left(k \cdot D - \frac{2}{l_{12}}\right)\alpha_7 + k \cdot E\alpha_8 + \left(k \cdot F + \frac{2}{l_{31}}\right)\alpha_9 \\ \varphi_2 = -\frac{1}{2}\alpha_3 + \frac{1}{2}\alpha_5 + \left(k \cdot D + \frac{2}{l_{12}}\right)\alpha_7 + \left(k \cdot E - \frac{2}{l_{23}}\right)\alpha_8 + k \cdot F\alpha_9 \\ \varphi_3 = -\frac{1}{2}\alpha_3 + \frac{1}{2}\alpha_5 + k \cdot D\alpha_7 + \left(k \cdot E + \frac{2}{l_{23}}\right)\alpha_8 + \left(k \cdot F - \frac{2}{l_{31}}\right)\alpha_9 \end{cases} \tag{52}$$

Compared to the nodal rotations in equation (32), we can rewrite equation (52) as:

$$\begin{cases} \varphi_1 = \varphi_R + \varphi_{P1} + k \cdot D\alpha_7 + k \cdot E\alpha_8 + k \cdot F\alpha_9 \\ \varphi_2 = \varphi_R + \varphi_{P2} + k \cdot D\alpha_7 + k \cdot E\alpha_8 + k \cdot F\alpha_9 \\ \varphi_3 = \varphi_R + \varphi_{P3} + k \cdot D\alpha_7 + k \cdot E\alpha_8 + k \cdot F\alpha_9 \end{cases} \tag{53}$$

which permits the following expression of the nodal drilling rotations:

$$\varphi_i = \varphi_R + \varphi_{Pi} + \psi \tag{54}$$

with $\psi = k \cdot D\alpha_7 + k \cdot E\alpha_8 + k \cdot F\alpha_9$ in which, ψ is a rotational term that appears after applying the constraint of equation (45).

The important question here is: Does the additional rotation ψ that appears in the above expression of the rotational *DOFs* affect the value of the true nodal drilling rotation before applying the constraint? To answer that question, let us examine the constraint we have imposed onto the solution of equation (31).

According to equation (48), we can write:

$$\begin{cases} P_4 = \alpha_7 = \frac{-l_{12}}{6}\varphi_1 + \frac{l_{12}}{6}\varphi_2 \\ P_5 = \alpha_8 = \frac{-l_{23}}{6}\varphi_2 + \frac{l_{23}}{6}\varphi_3 \\ P_6 = \alpha_9 = \frac{l_{31}}{6}\varphi_1 - \frac{l_{31}}{6}\varphi_3 \end{cases} \tag{55}$$

Which makes:

$$\frac{1}{l_{12}}\alpha_7+\frac{1}{l_{23}}\alpha_8+\frac{1}{l_{31}}\alpha_9 = \frac{1}{l_{12}}\left(\frac{-l_{12}}{6}\varphi_1+\frac{l_{12}}{6}\varphi_2\right) + \frac{1}{l_{23}}\left(\frac{-l_{23}}{6}\varphi_2+\frac{l_{23}}{6}\varphi_3\right)+\frac{1}{l_{31}}\left(\frac{l_{31}}{6}\varphi_1-\frac{l_{31}}{6}\varphi_3\right)=0 \tag{56}$$

Hence, the additional rotational term ψ that appears in the expression of the nodal rotation is absolutely zero. Then we obtain $\varphi_i = \varphi_R + \varphi_{Pi}$ which is absolutely the true drilling rotational DOF.

One would expect that the nodal rotations φ_i are the nodal values of the rotational field given in equation B5 and equation B6 when evaluated at nodal points (x_i, y_i). However, when equation B5 or equation B6 is evaluated at point $(x_1, y_1) = (0, 0)$ for example, it seems that φ_1 does not equal to $\varphi_R + \varphi_{P1}$ because contributions from φ_2 and φ_3 apparently arise. Nevertheless, substituting $(x = 0, y = 0)$ in equation B6 gives:

$$\varphi_1 = \frac{1}{2x_2y_3}(u_1x_2 - u_1x_3 + u_2x_3 - u_3x_2 - v_1y_3 + v_2y_3) + \frac{1}{3x_2y_3}(\varphi_1 l_{12}y_3 - \varphi_2 l_{12}y_3 - \varphi_1 C_{31}l_{31}x_2 + \varphi_3 C_{31}l_{31}x_2) \tag{57}$$

which can be rewritten as:

$$\varphi_1 = \frac{1}{2x_2y_3}(u_1x_2 - u_1x_3 + u_2x_3 - u_3x_2 - v_1y_3 + v_2y_3) + \frac{l_{12}y_3}{3x_2y_3}(\varphi_1 - \varphi_2) + \frac{C_{31}l_{31}x_2}{3x_2y_3}(\varphi_3 - \varphi_1) \tag{58}$$

Having in mind that: $\alpha_7 = \frac{l_{12}}{6}(\varphi_2 - \varphi_1)$, and $\alpha_9 = \frac{l_{31}}{6}(\varphi_1 - \varphi_3)$, we can write the above equality as:

$$\varphi_1 = \frac{1}{2x_2y_3}(u_1x_2 - u_1x_3 + u_2x_3 - u_3x_2 - v_1y_3 + v_2y_3) + \frac{2}{x_2}\frac{l_{12}}{6}(\varphi_1 - \varphi_2) + \frac{2C_{31}}{y_3}\frac{l_{31}}{6}(\varphi_3 - \varphi_1) \tag{59}$$

After substitution, we get:

$$\varphi_1 = \varphi_R - \frac{2}{x_2}\alpha_7 + \frac{2C_{31}}{y_3}\alpha_9 \tag{60}$$

In our case, $x_2 = l_{12}$ and $C_{31} \times l_{31} = y_3$, which yields $-\frac{2}{x_2}\alpha_7 + \frac{2C_{31}}{y_3}\alpha_9 = -\frac{2}{l_{12}}\alpha_7 + \frac{2}{l_{31}}\alpha_9 = \varphi_{P1}$.

Hence, we get $\varphi_1 = \varphi_R + \varphi_{P1}$.

Similarly, equation B5 or equation B6 yields $\varphi_2 = \varphi_R + \varphi_{P2}$ and $\varphi_3 = \varphi_R + \varphi_{P3}$ when evaluated at the two other nodal points (x_2, y_2) and (x_3, y_3), respectively.

5. Spurious zero-energy mode

Owing to the quadratic interpolation of the displacement field, the present element has a spurious zero energy mode corresponds to: $\varphi_1 = \varphi_2 = \varphi_3$, which results in a rank deficiency of the stiffness matrix. This is because of equation (55), which implies that $\varphi_1 = \varphi_2 = \varphi_3$ will provide zero-strain state. However, zero-energy mode control procedures can be applied (MacNeal and Harder, 1988). In this purpose, we introduce an additional condition, that makes the configuration $\varphi_1 = \varphi_2 = \varphi_3 = \phi_R$ provides a non-zero-strain state. The stabilization procedure lies in the following equality:

$$\phi_R = \varphi(x_0, y_0) = \frac{\varphi_1 + \varphi_2 + \varphi_3}{3} = -\frac{1}{2}\alpha_3 + \frac{1}{2}\alpha_5 \tag{60}$$

Our methodology consists of considering that, on the first hand; the rigid body rotation $\phi_R = \frac{1}{3}(\varphi_1 + \varphi_2 + \varphi_3)$ will produce some quantity of non-zero strains. On the other hand, this stain will be eliminated by adding an opposite strain (of the same quantity but with negative sign) because of the rigid body rotation $\phi_R = -\frac{1}{2}\alpha_3 + \frac{1}{2}\alpha_5$.

Once again, this condition must preserve the integrity of the true drilling rotational quantities. Thus, the strain quantity that will be added and then subtracted must provide zero nodal rotations in both cases.

According to equation (32), any non-zero additional strain that provides zero nodal rotations must be owing to a set of mid-side normal displacements that satisfies $\frac{1}{l_{12}}\alpha_7 = \frac{1}{l_{23}}\alpha_8 = \frac{1}{l_{31}}\alpha_9$.

To achieve this purpose, let us consider the following equation:

$$\begin{cases} \overline{\alpha_7} = l_{12}\left(\frac{1}{3}(\varphi_1 + \varphi_2 + \varphi_3) - \left(-\frac{1}{2}\alpha_3 + \frac{1}{2}\alpha_5\right)\right) \\ \overline{\alpha_8} = l_{23}\left(\frac{1}{3}(\varphi_1 + \varphi_2 + \varphi_3) - \left(-\frac{1}{2}\alpha_3 + \frac{1}{2}\alpha_5\right)\right) \\ \overline{\alpha_9} = l_{31}\left(\frac{1}{3}(\varphi_1 + \varphi_2 + \varphi_3) - \left(-\frac{1}{2}\alpha_3 + \frac{1}{2}\alpha_5\right)\right) \end{cases} \tag{61}$$

In matrix form:

$$\{\overline{\alpha}\} = [\overline{H}]\{U\} \tag{62}$$

According to equation (60), we can write:

$$\frac{1}{3}(\varphi_1 + \varphi_2 + \varphi_3) - \left(-\frac{1}{2}\alpha_3 + \frac{1}{2}\alpha_5\right) = 0 \tag{63}$$

Then, we have:

$$[\overline{H}]\{U\} = 0 \tag{64}$$

Equation (61), represents the additional condition that will be added to the elemental equilibrium equation to stabilize the spurious zero-energy mode.

Finally, the stabilized stiffness matrix will be:

$$[K] = [K_0] + \gamma GV[\overline{H}]^T[\overline{H}] \tag{65}$$

with G is the shear modulus, V is the element's volume and γ is a dimensionless constant.

In this work, the penalty parameter γ is taken to be 10^{-4} to neutralize its effect on the convergence properties of the rotational field.

6. Numerical validation

The correctness of the drilling rotational quantities used in this formulation is shown throughout the paper, and does not require numerical validation. However, we have performed this numerical validation in the objective to check the feasibility of the proposed methods. In this section, the numerical results obtained by the present formulation are compared against those by the standard Allman's triangular element to show that the response in terms of rotations obtained by elements with vertex rotations does not converge to the true drilling rotation solution even with mesh refinement.

As expected, the presented element exhibits the same order of convergence of nodal displacements as for Allman's triangle because both elements use the same order of interpolation. However, and most importantly, they exhibit different behaviours of rotational field convergence as shown in Tables IV-VI.

The values of drilling rotations at corner nodes of all elements in the mesh of the presented examples satisfy the following relation with Allman's vertex rotations presented in Allman (1984) as:

$$\varphi_i - \varphi_0 = 3/4(\omega_i - \omega_0) \tag{66}$$

in which, φ_0, and ω_0 stand for the average drilling rotation and average vertex rotation, respectively.

Note that it is not the aim of the present work to enhance the convergence rate of the presented finite element. The main goal is to get the true drilling rotational field. Then, all technics that have been used to improve performances of membrane elements with the linked interpolation can be applied to the present formulation to improve numerical performances with true drilling rotation.

The main finding of the present work is the kinematic relation linking the mid-side lateral displacement to corner node drilling rotations presented in equation (55), which is obviously dependent on the quality of the constraint adopted to remove singularity of the transformation matrix in equation (31). In this work, the kinematic relations in equation (55) are obtained by applying the inter-element compatibility condition. Other conditions can be investigated, and other relations can be established between the mid-side lateral displacements and corner node true drilling rotations if other constraints are adopted, such as equilibrium or energy conditions. In addition, investigating other constraints could yield in elements with better convergence rate using true drilling rotational DOFs.

6.1 Single-element eigenvalue test

The first benchmark refers to eigenvalues analyses of one element stiffness matrix (K^e) to detect the presence of spurious modes and assess the effectiveness of the stabilization operator. Membrane finite elements must have three rigid-body modes on an element without constraints. Therefore, only three of the eigenvalues should be zero for a full-rank membrane element's stiffness matrix.

The single element model has unit side length and thickness. The material properties are assumed to be $E = 1.0$ and $\nu = 0.3$. According to the numerical results reported in Table I, the element exhibits only three zero eigenvalues associated with the three rigid modes, which confirm that the stiffness matrix is rank sufficient.

6.2 The twisting test

In this test, a square plate discretised into four triangular elements as shown in Figure 4 is subject to four different solicitations to check its ability to correctly undertake in-plane twist (Shang *et al.*, 2018). The elastic proprieties are: $E = 10^6$, $v = 0.25$, and thickness $h = 0.01$.
The four solicitation cases are as follows:

(1) Make $u_1 = v_1 = 0$ and $\varphi_1 = 0.1$ at node (1).

(2) Make $u_1 = v_1 = 0$ at node (1) and $v_2 = 0.1$ at node (2).

(3) Make $u_1 = v_1 = \varphi_1 = 0$ at node (1) and apply a pair of opposite forces $P = 5$ at nodes (2) and (4), respectively [Figure 4 (b)].

(4) Make $u_1 = v_1 = u_4 = 0$ and apply a twisting moment $m = 5$ at the central node (1) [Figure 4 (c)].

λ_i	Eigenvalue
1	1.2372
2	0.7172
3	0.7172
4	0.0221
5	0.0221
6	0.000087
7	−3.6572 E-17
8	4.9593 E-17
9	4.9593 E-17

Table I.
Eigenvalues of the single element model

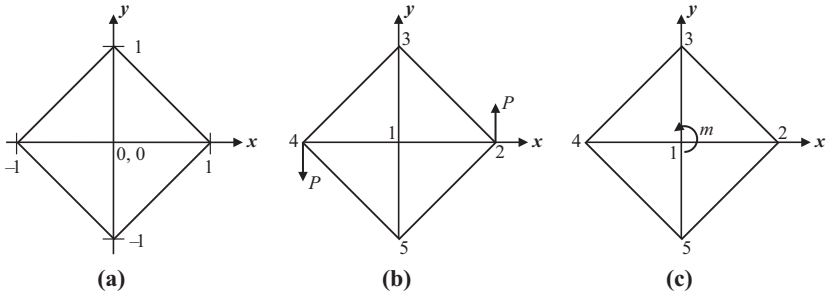

Figure 4.
The twisting test

The first two cases will produce a rigid body rotation with constant rotational angle of 0.1.

For the last two cases, the reaction moment M_1 on Node (1) is measured for Case 3, and the reaction force F_{y4} acting on Node (4) is measured for Case 4. The obtained results are listed in Table II and Table III along with the reference solution. It is obvious that the present element is able to obtain exact solutions for all studied cases.

6.3 Cantilever beam under a tip load

In this example, the cantilever beam of rectangular cross-section shown in Figure 5 is studied. The left end of the beam is fixed, and a parabolic shear distribution is applied at the right end. The dimensions and elastic properties of the beam are $L = 48$, $h = 12$, $b = 1$, $E = 3 \times 10^4$ and $\nu = 0.25$. The tip displacements and rotations obtained by the presented triangular element are given in Table IV against those obtained using Allman's triangle (Allman, 1984).

The reference solution to this problem is the analytical solution derived from two-dimensional elasticity given by (Timoshenko and Goodier, 1970) as follows:

$$u = \frac{-P}{6EI}\left(y - \frac{h}{2}\right)\left[(6L - 3x)x + (2 + \nu)\left(y^2 - hy\right)\right] \tag{67}$$

Table II.
Nodal displacements and rotations of the twisting test: Cases 1 and 2

	Case 1			Case 2		
Node	U	V	φ	U	V	φ
1	0.0	0.0	0.1	0.0	0.0	0.1
2	0.0	0.1	0.1	0.0	0.1	0.1
3	−0.1	0.0	0.1	−0.1	0.0	0.1
4	0.0	−0.1	0.1	0.0	−0.1	0.1
5	0.1	0.0	0.1	0.1	0.0	0.1

Table III.
Reaction forces of the twisting test: Cases 3 and 4

	Case 3	Case 4
Reaction	M1	Fy4
Numerical	10.00	5.0
Reference	10.00	5.0

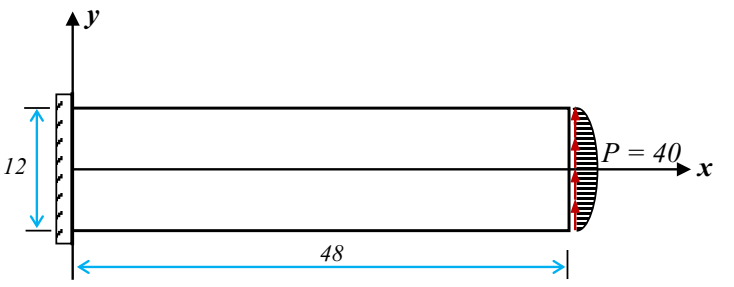

Figure 5.
Cantilever beam: geometry and loading

$$v = \frac{P}{6EI}\left[3\upsilon\left(y-\frac{h}{2}\right)^2(L-x)+\frac{1}{4}(4+5\upsilon)h^2x+(3L-x)x^2\right] \tag{68}$$

A simple numerical application gives the tip deflection: $v = 0.3553$.

The drilling rotation is calculated as:

$$\begin{aligned}\varphi = \frac{1}{2}\left(\frac{\partial v}{\partial x}-\frac{\partial u}{\partial y}\right) &= \frac{P}{12EI}\left[-3\upsilon\left(y-\frac{h}{2}\right)^2+\frac{1}{4}(4+5\upsilon)h^2+6Lx-3x^2\right] \\ &+\frac{P}{12EI}\left[\left(y-\frac{h}{2}\right)(2+\upsilon)(2y-h)+(2+\upsilon)\left(y^2-hy\right)+6Lx-3x^2\right]\end{aligned} \tag{69}$$

The numerical application gives the exact solution for the tip drilling rotation as $\varphi = 0.01253$.

To check the correctness of the obtained rotational DOFs, we need to prevent any dependent effect of the penalty parameter of the stabilisation matrix on the results. That is why the stabilisation factor is not considered in this example.

The results shown in Table IV, give a clear numerical confirmation of the correctness of the drilling rotational DOF of the present formulation, while Allman's rotational DOF converges toward an incorrect solution even with mesh refinement.

6.4 Cook's problem

In this test, a tapered cantilever beam of unit thickness shown in Figure 6, is clamped on one end and subjected to a distributed shear load on the other end. The elastic proprieties are: $E = 1$, $\upsilon = 1/3$. The obtained results listed in Table V show the clear difference between the vertex rotation of Allman's element and the drilling rotation of the present formulation.

6.5 Pure bending test

A cantilever beam subjected to pure bending is considered in this test. The dimensions of the beam are the length $L = 10$, width $b = 1$, and thickness $h = 2$. The elastic properties are Young's modulus $E = 1500$, Poisson's ratio $\upsilon = 0$. Two different loading cases are considered, whereby the bending moment is applied by two forces (load case 1 with $P = 1$) or by two nodal couples (Load Case 2 with $m = 0.5$) as shown in Figure 7. The computed end rotation and vertical deflection of the free end are listed in Table VI.

The obtained numerical results of the analysis are compared to the beam theory exact solution of 1.0 for vertical displacement and 0.2 for end rotation.

For Load Case 1, it is clear that the present element exhibits better convergence behaviour towards the reference solution of true drilling rotation, while Allman's element

Mesh	Tip vertical displacement		Tip rotation	
	Present	Allman	Present	Allman
1 × 4	0.2696	0.2696	−9.725e-3	−1.297e-2
2 × 8	0.3261	0.3261	−1.197e-2	−1.597e-2
4 × 16	0.3471	0.3471	−1.247e-2	−1.662e-2
8 × 32	0.3536	0.3536	−1.263e-2	−1.684e-2
16 × 64	0.3554	0.3554	−1.256e-2	−1.675e-2
Exact	0.3553		1.253e-2	

Table IV.
Cantilever beam: tip displacement and rotation

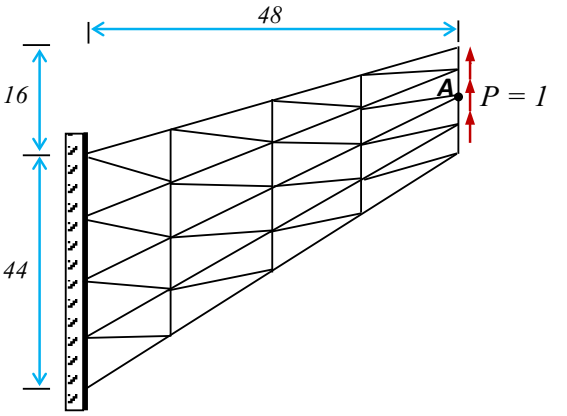

Figure 6.
Cook's cantilever beam: geometry, mesh and loading

Table V.
Cook's cantilever beam: tip displacement and rotation

	Tip vertical displacement		Tip rotation	
Mesh	Present	Allman	Present	Allman
4×4	22.415	22.415	−0.7002	−0.9337
8×8	23.453	23.453	−0.7221	−0.9628
16×16	23.805	23.805	−0.7329	−0.9772
32×32	23.919	23.919	−0.7381	−0.9841
Reference	23.96		/	

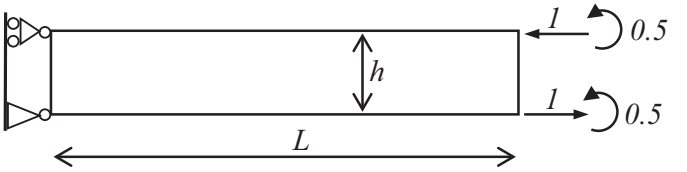

Figure 7.
Cantilever beam under pure bending

converges towards a wrong value even with mesh refinement. However, for Load Case 2, which is not a consistent loading, the computed rotations are wrong. The excessive rotation field is due to the need to restrain the spurious singular rotation mode when a concentrated moment is applied at a drilling DOF.

7. Conclusion

A displacement based formulation for membrane elements with true drilling rotation is proposed. The presented formulation can be applied to triangular and quadrilateral elements. In this work, we have described the construction of a compatible triangular element with nine DOFs starting from the *LST's* complete quadratic displacement field with 12 *DOFs*. The element incorporates the true drilling rotational DOFs into the displacement field interpolation without any presumed geometric transformations, with the help of the polynomial interpolation.

The present investigation provides the correct relation between the in-plane drilling rotational DOFs and the mid-side normal displacement. This corrected liked interpolation

Mesh	Load case	Present		Allman	
		Tip vertical displacement	Tip rotation	Tip vertical displacement	Tip rotation
4×1	1	0.7053	0.1501	0.7054	0.1765
	2	0.7423	0.8559	0.8330	13.6229
8×2	1	0.9173	0.1954	0.9165	0.2600
	2	0.9922	0.5452	1.3185	0.9875
16×4	1	0.9816	0.2052	0.9805	0.2690
	2	1.0694	1.5003	1.3979	2.3146
32×8	1	1.0065	0.2089	1.0053	0.2615
	2	1.1048	4.8789	1.3734	7.3468
Exact		1	0.2	1	0.2

Table VI.
Cantilever beam under pure bending: tip displacement and rotation

can be also applied to quadrilateral elements to get elements with true drilling rotation. Moreover, the proposed triangular element provides an explicit bilinear expression of the rotational field that represents the true drilling rotation provided by continuum mechanics. However, the presented element exhibits a spurious zero-energy mode similar to that of Allman's element. An effective strategy that removes the spurious modes while preserving true drilling rotational field is presented.

The obtained numerical results demonstrate the consistency of the present formulation with the rotational "skew-symmetric" component provided by continuum mechanics. Therefore, the presented element can be correctly coupled with other engineering elements with rotational DOFs. Moreover, the numerical comparison shows that the vertex rotation response does not converge to the solution of true drilling rotation even with mesh refinement.

Note that it is not the aim of the present work to enhance the convergence rate of the presented finite element. To improve the element's numerical behaviour, all techniques based on Allman's interpolation can be directly applied to the present element. Hence, the present element can replace Allman's concept to be the theoretical support for the development of several triangular and quadrangular membrane and shell elements. Furthermore, it can be a good candidate for commercial software.

References

Allman, D.J. (1984), "A compatible triangular element including vertex rotations for plane elasticity analysis", *Computers and Structures*, Vol. 19 Nos 1/2, pp. 1-8.

Allman, D.J. (1988), "Quadrilateral finite element including vertex rotations for plane elasticity analysis", *International Journal for Numerical Methods in Engineering*, Vol. 26 No. 3, pp. 717-730.

Allman, D.J. (1993), "Variational validation of a membrane finite element with drilling rotations", *Communications in Numerical Methods in Engineering*, Vol. 9 No. 4, pp. 345-351.

Bathe, K.J. and Ho, L.W. (1981), "A simple and effective element for analysis of general shell structures", *Computers and Structures*, Vol. 13 Nos 5/6, pp. 673-681.

Belarbi, M.T. and Bourezane, M. (2005), "On improved Sabir triangular element with drilling rotation", *Revue Européenne de Genie Civil*, Vol. 9 Nos 9/10, pp. 1151-1175.

Bergan, P.G. and Felippa, C.A. (1985), "A triangular membrane element with rotational degrees of freedom", *Computer Methods in Applied Mechanics and Engineering*, Vol. 50 No. 1, pp. 25-69.

Bergan, P.G. and Nygård, M.K. (1984), "Finite elements with increased freedom in choosing shape functions", *International Journal for Numerical Methods in Engineering*, Vol. 20 No. 4, pp. 643-664.

Boutagouga, D. (2017), "A new enhanced assumed strain quadrilateral membrane element with drilling degree of freedom and modified shape functions", *International Journal for Numerical Methods in Engineering*, Vol. 110 No. 6, pp. 573-600.

Boutagouga, D. and Djeghaba, K. (2016), "Nonlinear dynamic co-rotational formulation for membrane elements with in-plane drilling rotational degree of freedom", *Engineering Computations*, Vol. 33 No. 3, pp. 667-697.

Carpenter, N., Stolarski, H. and Relytschko, T. (1985), "A flat triangular shell element with improved membrane interpolation", *Communications in Applied Numerical Methods*, Vol. 1 No. 4, pp. 161-168.

Cazzani, A. and Atluri, S.N. (1993), "Four-noded mixed finite elements, using unsymmetric stresses, for linear analysis of membranes", *Computational Mechanics*, Vol. 11 No. 4, pp. 229-251.

Cen, S., Zhou, M.J. and Fu, X.R. (2011), "A 4-node hybrid stress-function (HS-F) plane element with drilling degrees of freedom less sensitive to severe mesh distortions", *Computers and Structures*, Vol. 89 Nos 5/6, pp. 517-528.

Choi, N., Choo, Y.S. and Lee, B.C. (2006), "A hybrid trefftz plane elasticity element with drilling degrees of freedom", *Computer Methods in Applied Mechanics and Engineering*, Vol. 195 Nos 33/36, pp. 4095-4105.

Cook, R.D. (1986), "On the Allman triangle and a related quadrilateral element. Computers and structures", *Computers and Structures*, Vol. 22, pp. 1065-1067.

Cook, R.D. (1987), "A plane hybrid element with rotational D.O.F and adjustable stiffness", *International Journal for Numerical Methods in Engineering*, Vol. 24 No. 8, pp. 1499-1508.

Cook, R.D. (1990), "Some options for plane triangular elements with rotational degrees of freedom", *Finite Elements in Analysis and Design*, Vol. 6 No. 3, pp. 245-249.

Cook, R.D. (1991), "Modified formulations for nine D.O.F plane triangles that include vertex rotations", *International Journal for Numerical Methods in Engineering*, Vol. 31 No. 5, pp. 825-835.

Cook, R.D. (1993), "Further development of a three-node triangular shell element", *International Journal for Numerical Methods in Engineering*, Vol. 36 No. 8, pp. 1413-1425.

Cook, R.D. (1994), "Four-node `flat' shell element: drilling degrees-of-freedom, membrane-bending coupling, warped geometry, and behavior", *Computers Structures*, Vol. 50 No. 4, pp. 549-555.

Felippa, C.A. (2003), "Study of optimal membrane triangles with drilling freedoms", *Computer Methods in Applied Mechanics and Engineering*, Vol. 192 Nos 16/18, pp. 2125-2168.

Geyer, S. and Groenwold, A.A. (2002), "Two hybrid stress membrane finite element families with drilling rotations", *International Journal for Numerical Methods in Engineering*, Vol. 53 No. 3, pp. 583-601.

Hughes, T.J.R. and Brezzi, F. (1989), "On drilling degrees of freedom", *Computer Methods in Applied Mechanics and Engineering*, Vol. 72 No. 1, pp. 105-121.

Ibrahimbegovic, A. (1993), "Mixed finite element with drilling rotations for plane problems in finite elasticity", *Computer Methods in Applied Mechanics and Engineering*, Vol. 107, pp. 225-238.

Ibrahimbegovic, A. and Frey, F. (1992), "Quadrilateral membrane elements with rotational degrees of freedom", *Engineering Fractional Mechanics*, Vol. 43, pp. 13-24.

Ibrahimbegovic, A. and Wilson, E.L. (1991), "A unifed formulation for triangular and quadrilateral flat shell finite element with six nodal degrees of freedom", *Communications in Applied Numerical Methods*, Vol. 7 No. 1, pp. 1-9.

Ibrahimbegovic, A., Taylor, R.L. and Wilson, E.L. (1990), "A robust quadrilateral membrane finite element with drilling degrees of freedom", *International Journal for Numerical Methods in Engineering*, Vol. 30 No. 3, pp. 445-457.

Iura, M. and Atluri, S.N. (1992), "Formulation of a membrane finite element with drilling degrees of freedom", *Computational Mechanics*, Vol. 96, pp. 417-428.

Jaamei, S., Frey, F. and Jetteur, P. (1989), "Nonlinear thin shell finite element with six degrees of freedom per node", *Computer Methods in Applied Mechanics and Engineering*, Vol. 75 Nos 1/3, pp. 251-266.

Kugler, S., Fotiu, P. and Murin, J. (2010), "A highly efficient membrane finite element with drilling degrees of freedom", *Acta Mechanica*, Vol. 213 Nos 3/4, pp. 323-348.

MacNeal, R.H. (1989), "Toward a defect-free four nodded membrane element", *Finite Elements in Analysis and Design*, Vol. 5 No. 1, pp. 31-37.

MacNeal, R.H. and Harder, R.L. (1988), "A refined four-node membrane element with rotational degrees of freedom", *Computers Structures*, Vol. 28 No. 1, pp. 75-84.

Madeo, A., Zagari, G. and Casciaro, R. (2012), "An isostatic quadrilateral membrane finite element with drilling rotations and no spurious modes", *Finite Elements in Analysis and Design*, Vol. 50, pp. 21-32.

Madeo, A., Casciaro, R., Zagari, G., Zinno, R. and Zucco, G. (2014), "A mixed isostatic 16 dof quadrilateral membrane element with drilling rotations, based on airy stresses", *Finite Elements in Analysis and Design*, Vol. 89, pp. 52-66.

Nodargi, N.A., Caselli, F., Artioli, E. and Bisegna, P. (2016), "A mixed tetrahedral element with nodal rotations for large-displacement analysis of inelastic structures", *International Journal for Numerical Methods in Engineering*, Vol. 108 No. 7, pp. 722-749.

Pawlak, T.P., Yunus, S.M. and Cook, R.D. (1991), "Solid elements with rotational degrees of freedom: part II-tetrahedron elements", *International Journal for Numerical Methods in Engineering*, Vol. 31 No. 3, pp. 593-610.

Piltner, R. and Taylor, R.L. (1995), "A quadrilateral mixed finite element with two enhanced strain modes", *International Journal for Numerical Methods in Engineering*, Vol. 38 No. 11, pp. 1783-1808.

Piltner, R. and Taylor, R.L. (2000), "Triangular finite elements with rotational degrees of freedom and enhanced strain modes", *Computers and Structures*, Vol. 75, pp. 361-368.

Pimpinelli, G. (2004), "An assumed strain quadrilateral element with drilling degrees of freedom", *Finite Elements in Analysis and Design*, Vol. 41 No. 3, pp. 267-283.

Rebiai, C. and Belounar, L. (2013), "A new strain based rectangular finite element with drilling rotation for linear and nonlinear analysis", *Archives of Civil and Mechanical Engineering*, Vol. 13 No. 1, pp. 72-81.

Rebiai, C. and Belounar, L. (2014), "An effective quadrilateral membrane finite element based on the strain approach", *Measurement*, Vol. 50, pp. 263-269.

Rezaiee-Pajand, M.P. and Karkon, M. (2013), "An effective membrane element based on analytical solution", *European Journal of Mechanics A/Solids*, Vol. 39, pp. 268-279.

Rezaiee-Pajand, M. and Yaghoobi, M. (2017), "A hybrid stress plane element with strain field", *Civil Engineering Infrastructures Journal*, Vol. 50 No. 2, pp. 255-275.

Sabir, A.B. (1985), "A rectangular and triangular plane elasticity element with drilling degrees of freedom", *Chapter 9 in Proceeding of the 2nd International Conference on Variational Methods in Engineering*, Southampton University, Springer-Verlag, Berlin, pp. 17-25.

Shang, Y. and Ouyang, W. (2018), "4-Node unsymmetric quadrilateral membrane element with drilling DOFs insensitive to severe mesh-distortion", *International Journal for Numerical Methods in Engineering*, Vol. 113 No. 10, pp. 1589-1606.

Shang, Y., Cen, S., Qian, Z.-H. and Li, C. (2018), "High-performance unsymmetric 3-node triangular membrane element with drilling DOFs can correctly undertake in-plane moments", *Engineering Computations*, Vol. 35 No. 7, pp. 2543-2556.

Simo, J.C., Fox, D.D. and Hughes, T.J.R. (1992), "Formulation of finite elasticity with independent rotations", *Comp. Meth. Appl. Mech. Eng*, Vol. 95 No. 2, pp. 277-288.

Sze, K.Y. and Pan, Y.S. (2000), "Hybrid stress tetrahedral elements with Allman's rotational D.O.F.s", *International Journal for Numerical Methods in Engineering*, Vol. 48 No. 7, pp. 1055-1070.

Sze, K.Y., Soh, A.K. and Sim, Y.S. (1996), "An explicit hybrid-stabilized solid element with rotational degrees of freedom", *International Journal for Numerical Methods in Engineering*, Vol. 39 No. 17, pp. 2987-3005.

Sze, K.Y., Wanji, C. and Cheung, Y.K. (1992), "An efficient quadrilateral plane element with drilling degrees of freedom using orthogonal stress modes", *Computational Structures*, Vol. 42 No. 5, pp. 695-705.

Timoshenko, S.P. and Goodier, J.N. (1970), *Theory of Elasticity*, 3rd ed., McGraw Hill, New York, NY.

To, C.W.S. and Liu, M.L. (1994), "Hybrid strain based three-node flat triangular shell elements", *Finite Elements in Analysis and Design*, Vol. 17 No. 3, pp. 169-203.

Wisniewski, K. and Turska, E. (2006), "Enhanced Allman quadrilateral for finite drilling rotations", *Computer Methods in Applied Mechanics and Engineering*, Vol. 195 Nos 44/47, pp. 6086-6109.

Wisniewski, K. and Turska, E. (2008), "Improved four-node Hellingere Reissner elements based on skew coordinates", *International Journal for Numerical Methods in Engineering*, Vol. 76 No. 6, pp. 798-836.

Wisniewski, K. and Turska, E. (2009), "Improved 4-node Hu-Washizu elements based on skew coordinates", *Computers and Structures*, Vol. 87 Nos 7/8, pp. 407-424.

Xing, C. and Zhou, C. (2016), "A singular planar element with rotational degree of freedom for fracture analysis", *Theoretical and Applied Fracture Mechanics*, Vol. 86, pp. 239-249.

Yunus, S.M., Pawlak, T.P. and Cook, R.D. (1991), "Solid elements with rotational degrees of freedom: part I-hexahedron elements", *International Journal for Numerical Methods in Engineering*, Vol. 31 No. 3, pp. 573-592.

Zienkiewicz, O.C. (1977), *The Finite Element Method*, 3rd ed., London Mc Graw Hill, UK

Zienkiewicz, O.C., Parekh, C.J. and King, I.P. (1965), "Arch dams analysed by a linear finite element shell solution program", *In Proceeding* Symposium *on Theory of Arch Dams*, Southampton University, Pergamon Press, Oxford.

Zouari, W., Hammadi, F. and Ayad, R. (2016), "Quadrilateral membrane finite elements with rotational DOFs for the analysis of geometrically linear and nonlinear plane problems", *Computers and Structures*, Vol. 173, pp. 139-149.

Appendix 1

$H_{71} = \frac{1}{k} \cdot \frac{x_3 - x_2}{2Fl_{31}y_3 + 2Dl_{12}y_3 + 2El_{23}y_3}$	$H_{81} = \frac{l_{23}}{l_{12}} H_{71}$	$H_{91} = \frac{l_{31}}{l_{12}} H_{71}$
$H_{72} = \frac{1}{k} \cdot \frac{1}{2Fl_{31} + 2Dl_{12} + 2El_{23}}$	$H_{82} = \frac{l_{23}}{l_{12}} H_{72}$	$H_{92} = \frac{l_{31}}{l_{12}} H_{72}$
$H_{73} = -\frac{2Fl_{12}l_{31} - 2l_{12} + El_{12}l_{23}}{6Fl_{31} + 6Dl_{12} + 6El_{23}}$	$H_{83} = \frac{-Fl_{23}l_{31} + 2l_{23} + Dl_{12}l_{23}}{6Fl_{31} + 6Dl_{12} + 6El_{23}}$	$H_{93} = \frac{2Dl_{12}l_{31} + 2l_{31} + El_{23}l_{31}}{6Fl_{31} + 6Dl_{12} + 6El_{23}}$
$H_{74} = \frac{1}{k} \cdot \frac{x_3}{2Fl_{31}y_3 + 2Dl_{12}y_3 + 2El_{23}y_3}$	$H_{84} = l_{23}H_{74}$	$H_{94} = l_{31}H_{74}$
$H_{75} = -H_{72}$	$H_{85} = -H_{82}$	$H_{95} = -H_{92}$
$H_{76} = \frac{2l_{12} + Fl_{12}l_{31} + 2El_{12}l_{23}}{6Fl_{31} + 6Dl_{12} + 6El_{23}}$	$H_{86} = -\frac{Fl_{23}l_{31} - 2l_{23} + 2Dl_{12}l_{23}}{6Fl_{31} + 6Dl_{12} + 6El_{23}}$	$H_{96} = \frac{2l_{31} - Dl_{12}l_{31} + El_{23}l_{31}}{6Fl_{31} + 6Dl_{12} + 6El_{23}}$
$H_{77} = \frac{1}{k} \cdot \frac{l_{12}}{2Fl_{31}y_3 + 2Dl_{12}y_3 + 2El_{23}y_3}$	$H_{87} = \frac{l_{23}}{l_{12}} H_{77}$	$H_{97} = \frac{l_{31}}{l_{12}} H_{77}$
$H_{78} = 0$	$H_{88} = 0$	$H_{98} = 0$
$H_{79} = \frac{2l_{12} + Fl_{12}l_{31} - El_{12}l_{23}}{6Fl_{31} + 6Dl_{12} + 6El_{23}}$	$H_{89} = \frac{2l_{23} + 2Fl_{23}l_{31} + Dl_{12}l_{23}}{6Fl_{31} + 6Dl_{12} + 6El_{23}}$	$H_{99} = -\frac{Dl_{12}l_{31} - 2l_{31} + 2El_{23}l_{31}}{6Fl_{31} + 6Dl_{12} + 6El_{23}}$

Table AI.
Elements of the [*H*] matrix

$H_{73} = -\frac{2Fl_{12}l_{31} + El_{12}l_{23}}{6Fl_{31} + 6Dl_{12} + 6El_{23}}$	$H_{83} = \frac{-Fl_{23}l_{31} + Dl_{12}l_{23}}{6Fl_{31} + 6Dl_{12} + 6El_{23}}$	$H_{93} = \frac{2Dl_{12}l_{31} + El_{23}l_{31}}{6Fl_{31} + 6Dl_{12} + 6El_{23}}$
$H_{76} = \frac{Fl_{12}l_{31} + 2El_{12}l_{23}}{6Fl_{31} + 6Dl_{12} + 6El_{23}}$	$H_{86} = -\frac{Fl_{23}l_{31} + 2Dl_{12}l_{23}}{6Fl_{31} + 6Dl_{12} + 6El_{23}}$	$H_{96} = \frac{-Dl_{12}l_{31} + El_{23}l_{31}}{6Fl_{31} + 6Dl_{12} + 6El_{23}}$
$H_{79} = \frac{Fl_{12}l_{31} - El_{12}l_{23}}{6Fl_{31} + 6Dl_{12} + 6El_{23}}$	$H_{89} = \frac{2Fl_{23}l_{31} + Dl_{12}l_{23}}{6Fl_{31} + 6Dl_{12} + 6El_{23}}$	$H_{99} = -\frac{Dl_{12}l_{31} + 2El_{23}l_{31}}{6Fl_{31} + 6Dl_{12} + 6El_{23}}$

Table AII.
Elements of the [*H*] matrix after simplification

Appendix 2

$$u = u_1 - \frac{x}{x_2}(u_1 - u_2) - \frac{y}{3x_2y_3}(3u_1x_2 - 3u_1x_3 + 3u_2x_3 - 3u_3x_2 - 2\varphi_1 C_{31} l_{31} x_2 + 2\varphi_3 C_{31} l_{31} x_2)$$
$$- \frac{xy}{3x_2y_3}(2\varphi_2 C_{23} l_{23} + 2\varphi_1 C_{31} l_{31} - 2\varphi_3 C_{23} l_{23} - 2\varphi_3 C_{31} l_{31})$$
$$- \frac{y^2}{3x_2y_3^2}(2\varphi_1 C_{31} l_{31} x_2 - 2\varphi_2 C_{23} l_{23} x_3 - 2\varphi_1 C_{31} l_{31} x_3 + 2\varphi_3 C_{23} l_{23} x_3 - 2\varphi_3 C_{31} l_{31} x_2 + 2\varphi_3 C_{31} l_{31} x_3) \tag{2.1}$$

$$u = u_1\left(1 - \frac{x}{x_2} - \frac{y}{x_2y_3}(x_2 - x_3)\right) + u_2\left(\frac{x}{x_2} - \frac{y}{x_2}\frac{x_3}{y_3}\right) + u_3\frac{y}{y_3}$$
$$- \varphi_1\left(\frac{1}{3}\frac{y^2}{x_2y_3^2}(2C_{31} l_{31} x_2 - 2C_{31} l_{31} x_3) - \frac{2}{3} y C_{31}\frac{l_{31}}{y_3} + \frac{2}{3} xy C_{31}\frac{l_{31}}{x_2y_3}\right)$$
$$- \varphi_2\left(\frac{2}{3} xy C_{23}\frac{l_{23}}{x_2y_3} - \frac{2}{3} y^2 C_{23}\frac{l_{23}}{x_2}\frac{x_3}{y_3^2}\right)$$
$$- \varphi_3\left(\frac{2}{3} y C_{31}\frac{l_{31}}{y_3} + \frac{1}{3}\frac{y^2}{x_2y_3^2}(2C_{23} l_{23} x_3 - 2C_{31} l_{31} x_2) - \frac{1}{3} x\frac{y}{x_2y_3^2}(2C_{23} l_{23} y_3 + 2C_{31} l_{31} y_3)\right) \tag{2.2}$$

$$v = v_1 - \frac{x}{3x_2^2}(3v_1x_2 - 3v_2x_2 - 2\varphi_1 l_{23} x_2 + 2\varphi_2 l_{23} x_2)$$
$$- \frac{y}{3x_2^2y_3}\begin{pmatrix} 3v_1x_2^2 - 3v_3x_2^2 - 3v_1x_2x_3 + 3v_2x_2x_3 + 2\varphi_1 l_{23} x_2 x_3 \\ -2\varphi_2 l_{23} x_2 x_3 - 2\varphi_1 S_{31} l_{31} x_2^2 + 2\varphi_3 S_{31} l_{31} x_2^2 \end{pmatrix}$$
$$- \frac{xy}{3x_2^2y_3}\begin{pmatrix} 2\varphi_1 l_{23} x_2 - 4\varphi_1 l_{23} x_3 - 2\varphi_2 l_{23} x_2 + 4\varphi_2 l_{23} x_3 \\ +2\varphi_2 S_{23} l_{23} x_2 + 2\varphi_1 S_{31} l_{31} x_2 - 2\varphi_3 S_{23} l_{23} x_2 - 2\varphi_3 S_{31} l_{31} x_2 \end{pmatrix} - \frac{x^2}{3x_2^2}(2\varphi_1 l_{23} - 2\varphi_2 l_{23})$$
$$- \frac{y^2}{3x_2^2y_3^2}\begin{pmatrix} 2\varphi_1 l_{23} x_3^2 - 2\varphi_2 l_{23} x_3^2 - 2\varphi_1 l_{23} x_2 x_3 + 2\varphi_2 l_{23} x_2 x_3 + 2\varphi_1 S_{31} l_{31} x_2^2 - 2\varphi_3 S_{31} l_{31} x_2^2 \\ -2\varphi_2 S_{23} l_{23} x_2 x_3 - 2\varphi_1 S_{31} l_{31} x_2 x_3 + 2\varphi_3 S_{23} l_{23} x_2 x_3 + 2\varphi_3 S_{31} l_{31} x_2 x_3 \end{pmatrix} \tag{2.3}$$

$$v = \frac{1}{3}\frac{v_1}{x_2^2 y_3}\left(3x_2^2 y_3 - 3yx_2^2 - 3xx_2 y_3 + 3yx_3 x_2\right) + \frac{v_2}{x_2^2 y_3}(xx_2 y_3 - yx_2 x_3) + \frac{v_3 y}{y_3}$$
$$- \frac{\varphi_1}{3x_2^2 y_3^2}\begin{pmatrix} 2x^2 l_{23} y_3^2 + 2y^2 l_{23} x_3^2 - 2xl_{23} x_2 y_3^2 - 2y^2 l_{23} x_2 x_3 + 2y^2 S_{31} l_{31} x_2^2 + 2yl_{23} x_2 x_3 y_3 \\ - 2y^2 S_{31} l_{31} x_2 x_3 - 2yS_{31} l_{31} x_2^2 y_3 + 2xyl_{23} x_2 y_3 - 4xyl_{23} x_3 y_3 + 2xyS_{31} l_{31} x_2 y_3 \end{pmatrix}$$
$$+ \frac{\varphi_2}{3x_2^2 y_3^2}\begin{pmatrix} 2x^2 l_{23} y_3^2 + 2y^2 l_{23} x_3^2 - 2xl_{23} x_2 y_3^2 - 2y^2 l_{23} x_2 x_3 + 2yl_{23} x_2 x_3 y_3 \\ + 2y^2 S_{23} l_{23} x_2 x_3 + 2xyl_{23} x_2 y_3 - 4xyl_{23} x_3 y_3 - 2xyS_{23} l_{23} x_2 y_3 \end{pmatrix}$$
$$+ \frac{\varphi_3}{3x_2^2 y_3^2}\left(2y^2 S_{31} l_{31} x_2^2 - 2y^2 S_{23} l_{23} x_2 x_3 - 2y^2 S_{31} l_{31} x_2 x_3 - 2yS_{31} l_{31} x_2^2 y_3 + 2xyS_{23} l_{23} x_2 y_3 + 2xyS_{31} l_{31} x_2 y_3\right) \tag{2.4}$$

$$\varphi = \frac{1}{6x_2 y_3}(3u_1 x_2 - 3u_1 x_3 + 3u_2 x_3 - 3u_3 x_2 - 3v_1 y_3 + 3v_2 y_3 + 2\varphi_1 l_{23} y_3 - 2\varphi_2 l_{23} y_3 - 2\varphi_1 C_{31} l_{31} x_2 + 2\varphi_3 C_{31} l_{31} x_2)$$
$$+ \frac{x}{3x_2^2 y_3}(2\varphi_2 l_{23} y_3 - 2\varphi_1 l_{23} y_3 + \varphi_2 C_{23} l_{23} x_2 + \varphi_1 C_{31} l_{31} x_2 - \varphi_3 C_{23} l_{23} x_2 - \varphi_3 C_{31} l_{31} x_2)$$
$$- \frac{y}{3x_2^2 y_3^2}\begin{pmatrix} \varphi_1 l_{23} x_2 y_3 - 2\varphi_1 l_{23} x_3 y_3 - \varphi_2 l_{23} x_2 y_3 + 2\varphi_2 l_{23} x_3 y_3 - 2\varphi_1 C_{31} l_{31} x_2^2 + 2\varphi_3 C_{31} l_{31} x_2^2 + 2\varphi_2 C_{23} l_{23} x_2 x_3 \\ + 2\varphi_1 C_{31} l_{31} x_2 x_3 - 2\varphi_3 C_{23} l_{23} x_2 x_3 - 2\varphi_3 C_{31} l_{31} x_2 x_3 + \varphi_2 S_{23} l_{23} x_2 y_3 + \varphi_1 S_{31} l_{31} x_2 y_3 - \varphi_3 S_{23} l_{23} x_2 y_3 - \varphi_3 S_{31} l_{31} x_2 y_3 \end{pmatrix} \tag{2.5}$$

$$\varphi = \frac{1}{2}\frac{u_1}{x_2 y_3}(x_2 - x_3) + \frac{1}{2}\frac{u_2}{x_2 y_3}x_3 - \frac{1}{2}\frac{u_3}{y_3} - \frac{1}{2}\frac{v_1}{x_2} + \frac{1}{2}\frac{v_2}{x_2}$$
$$- \varphi_1\left(\frac{1}{3x_2 y_3}(l_{23} y_3 - C_{31} l_{31} x_2) + \frac{x}{3x_2^2 y_3}(2l_{23} y_3 - C_{31} l_{31} x_2) + \frac{y}{3x_2^2 y_3^2}\left(l_{23} x_2 y_3 - 2C_{31} l_{31} x_2^2 - 2l_{23} x_3 y_3 + 2C_{31} l_{31} x_2 x_3 + S_{31} l_{31} x_2 y_3\right)\right)$$
$$- \varphi_2\left(\frac{l_{23}}{3x_2} - \frac{x}{3x_2^2 y_3}(2l_{23} y_3 + C_{23} l_{23} x_2) + \frac{y}{3x_2^2 y_3^2}(2l_{23} x_3 y_3 - l_{23} x_2 y_3 + 2C_{23} l_{23} x_2 x_3 + S_{23} l_{23} x_2 y_3)\right)$$
$$+ \varphi_3\left(\frac{C_{31} l_{31}}{3y_3} - \frac{x}{3x_2^2 y_3}(C_{23} l_{23} x_2 + C_{31} l_{31} x_2) + \frac{y}{3x_2^2 y_3^2}\left(2C_{23} l_{23} x_2 x_3 - 2C_{31} l_{31} x_2^2 + 2C_{31} l_{31} x_2 x_3 + S_{23} l_{23} x_2 y_3 + S_{31} l_{31} x_2 y_3\right)\right) \tag{2.6}$$

Corresponding author
Djamel Boutagouga can be contacted at: d.boutagouga@yahoo.fr